DOI: 10.1002/ecs2.3912

#### ARTICLE

Special Feature: Harnessing the NEON Data Revolution



# Exploring discrepancies between in situ phenology and remotely derived phenometrics at NEON sites

Alison Donnelly<sup>1</sup> | Rong Yu<sup>1,2,3</sup> | Katherine Jones<sup>4</sup> | Michael Belitz<sup>5</sup> |
Bonan Li<sup>6</sup> | Katharyn Duffy<sup>7</sup> | Xiaoyang Zhang<sup>8</sup> | Jianmin Wang<sup>8</sup> |
Bijan Seyednasrollah<sup>7</sup> | Katherine L. Gerst<sup>9,10</sup> | Daijiang Li<sup>11,12</sup> | |
Youssef Kaddoura<sup>13</sup> | Kai Zhu<sup>14</sup> | Jeffrey Morisette<sup>15</sup> | Colette Ramey<sup>16</sup>
Kathleen Smith<sup>16</sup>

<sup>2</sup>State Key Laboratory of Subtropical Silviculture, Zhejiang A&F University, Hangzhou, China

<sup>3</sup>Key Laboratory of Carbon Cycling in Forest Ecosystems and Carbon Sequestration of Zhejiang Province, Zhejiang A&F University, Hangzhou, China

<sup>4</sup>Battelle, National Ecological Observatory Network, Boulder, Colorado, USA

<sup>5</sup>Florida Museum of Natural History, University of Florida, Gainesville, Florida, USA

<sup>6</sup>Department of Biological and Ecological Engineering, Oregon State University, Corvallis, Oregon, USA

<sup>7</sup>School of Informatics, Computing and Cyber Systems, Northern Arizona University, Flagstaff, Arizona, USA

<sup>8</sup>Department of Geography, South Dakota State University, Brookings, South Dakota, USA

<sup>9</sup>School of Natural Resources and the Environment, University of Arizona, Flagstaff, Arizona, USA

<sup>10</sup>Bat Conservation International, Austin, Texas, USA

#### **Abstract**

In recent decades, the use of satellite sensors, near-surface cameras, and other remote methods for monitoring vegetation phenology at landscape and higher scales has become increasingly common. These technologies provide a means to determine the timing of phenophases and growing season length at different spatial resolutions; coverage that is not attainable by human observers. However, in situ ground observations are required to validate remotely derived phenometrics. Despite increased knowledge and expertise there still remains the persistent challenge of reconciling ground observations at the individual plant level with remotely sensed (RS) phenometrics at landscape or larger scales. We compared the timing of in situ phenophase estimates (spring and autumn) with a range of corresponding remote sensing (moderate resolution imaging spectroradiometer [MODIS], visible infrared imaging radiometer suite [VIIRS], PhenoCam) phenometrics across five terrestrial sites in the United States' NEON (Harvard Forest [MA] [HARV], Onaqui [UT] [ONAQ], Abby Road [WA] [ABBY], Disney Wilderness Preserve [FL] [DSNY], and Ordway-Swisher Biological Station [FL] [OSBS]) focusing on the 3-year period from 2017 to 2019. Our main objective was to explore potential reasons for the observed discrepancies between in situ and RS phenometrics and to determine which technologies were better able to capture ground observations. Statistically significant relationships were strongest (p < 0.001) for spring phenophases, while the only RS phenometrics significantly correlated with in situ estimates of autumn phenophases were leaf fall (p < 0.01) and leaves (p < 0.000). In particular, root mean square error (RMSE) (mean bias error

Any use of trade, firm, or product names is for descriptive purposes only and does not imply endorsement by the US government. The findings and conclusions in this paper are those of the authors and should not be construed to represent any official US Department of Agriculture, US Department of the Interior, or US government determination or policy.

This is an open access article under the terms of the Creative Commons Attribution License, which permits use, distribution and reproduction in any medium, provided the original work is properly cited.

© 2022 The Author(s). Ecosphere published by Wiley Periodicals LLC on behalf of The Ecological Society of America.

<sup>&</sup>lt;sup>1</sup>Department of Geography, University of Wisconsin-Milwaukee, Milwaukee, Wisconsin, USA

<sup>11</sup>Department of Biological Sciences, Louisiana State University, Baton Rouge, Louisiana, USA

<sup>12</sup>Center for Computation and Technology, Louisiana State University, Baton Rouge, Louisiana, USA

<sup>13</sup>Department of Wildlife Ecology and Conservation, University of Florida, Gainesville, Florida, USA

<sup>14</sup>Department of Environmental Studies, University of California, Santa Cruz, Santa Cruz, California, USA

<sup>15</sup>Department of the Interior, National Invasive Species Council, Fort Collins, Colorado, USA

<sup>16</sup>Department of Biology-Botany, Metropolitan State University of Denver, Denver, Colorado, USA

### Correspondence

Alison Donnelly Email: alison.c.donnelly@gmail.com

### **Funding information**

University of Wisconsin Milwaukee, Grant/Award Number: RGI 101x368; National Science Foundation; NEON Science Summit 2019 NSF Award, Grant/ Award Number: 1906144

Handling Editor: Jennifer Balch

[MBE]) for MODIS-Enhanced Vegetation Index-2 band (EVI2), VIIRS-EVI2, and PhenoCam-green chromatic coordinate (GCC) derived early spring transition dates indicated overall differences of 21.7 days (-4.6 days), 28.4 days (-1.2 days), and 24.1 days (11.9 days) from in situ estimates of early leaf-out dates. In autumn, RMSE/MBE was smallest (10.9 days/-2.2 days) between phenesse estimates (95th percentile date) of the latest date of in situ leaf fall and VIIRS derived end of senescence, compared to the equivalent phenometric derived from MODIS (13.5 days/7.7 days) and PhenoCam (GCC greenness-falling) (13.8 days/-5.1 days). Overall, discrepancies between in situ and RS phenology related to scale, species availability, and the short duration of the time series (3 years). However, as the NEON project progresses these challenges are expected to be reduced as more data become available.

#### KEYWORDS

in situ phenology, moderate resolution imaging spectroradiometer, NEON, Phenesse estimates, PhenoCam, Special Feature: Harnessing the NEON Data Revolution, visible infrared imaging radiometer suite

# INTRODUCTION

Understanding the role of vegetation phenology in determining the timing and duration of the carbon uptake period across different ecosystems is pivotal to the calculation of accurate carbon budgets for use in global ecosystem modeling (Richardson et al., 2010). The number and range of remote sensing (RS) methods used to determine the timing of phenophases and growing season length (GSL) have become increasingly common in recent years as a means to explore ecosystem dynamics, for use in C budget calculations and climate change research. These methods range from measures of (1) "greenness" from satellite data, digital repeat photography, and unmanned aerial vehicles to (2) estimations of photosynthetic activity based on C flux measurements and satellite-derived Fraction of Absorbed Photosynthetically Active Radiation (FAPAR) and Solar Induced Fluorescence (SIF). In addition, biophysical variables such as Leaf Area Index (LAI) and Fraction of Vegetation Cover (FCOVER) are also used. These methods provide an estimate of phenology over a relatively large geographical area that is not feasible by direct in situ observations. However, given the wide range of sensors (e.g., moderate resolution imaging spectroradiometer [MODIS], Satellite Pour l'Observation de la Terre [SPOT], visible infrared imaging radiometer suite [VIIRS], Sentinel), vegetation indices (e.g., Normalized Difference Vegetation Index [NDVI], Enhanced Vegetation Index [EVI]), and processes (C flux based phenology) being monitored and reported, not to mention scale, the challenge of reconciling in situ and RS determination of phenology persists.

In recent decades, changing environmental conditions, in particular climate has intensified interest in phenological research leading to a rapid growth in phenological data collection and processing from a range of sources including in situ, RS, and modeling (Donnelly & Yu, 2017; Fu et al., 2014; Richardson et al., 2009; Tang et al., 2016; Zhang et al., 2018a). Even with this increased knowledge and expertise there still remains the persistent challenge of reconciling ground observations at the individual plant level with remotely sensed phenometrics at the landscape or larger scale (Fu et al., 2014; Piao et al., 2019; Tang et al., 2016). However, some recently developed technologies, such as PhenoCams (Richardson et al., 2009) and unmanned aerial vehicles may, at least in part, help narrow the gap between in situ- and satellite-derived phenometrics.

In order to address this gap it is first necessary to understand some of the reasons behind its existence. A ECOSPHERE 3 of 25

review of the current literature revealed a wide range of factors contributing to discrepancies between in situ- and RS-derived phenometrics (Box 1 and Table 1). In general, in situ phenology was considered representative of local vegetation, in particular dominant trees, and when longterm (>30 years) records were available, correlation with climatic parameters was possible. However, correlating RS phenometrics with in situ data can be challenging as observations are generally made on a limited number of species (usually trees) covering a restricted geographical extent, usually close to population centers, typically confined to two seasons (spring and autumn) and recorded below the canopy. Other reported issues included, the subjective nature of in situ observations, which were often focused on the dominant species in the landscape, which may not be reflective of the overall vegetation within the RS field of view (FOV). Furthermore, data for which longterm observations were available (e.g., PEP725 network in Europe and the cloned lilac project in the United States) tended to be based on cloned plants which confound the issue of representativeness, while differences in definitions of phenophases between networks made crosscomparisons challenging. Other reported reasons for mismatches in the timing between satellite and in situ observations included (1) satellites observing the uppercanopy and observers monitoring from below; (2) speciesspecific canopy senescence patterns with some trees coloring from top to bottom or from extremities to the interior of the canopy; and (3) actual color of the leaves (yellow/red). Given the aforementioned issues validating a RS phenological signal becomes challenging.

As regards RS, whereas satellites provide large spatial coverage and high-frequency phenological data differences between sensors and the algorithms used to extract phenometrics can produce very different results (Bórnez et al., 2020). Discrepancies of up to 2 months between advanced very high-resolution radiometer (AVHRR) NDVI-start of season (SOS) and the timing of in situ phenology have been reported for North America depending on the retrieval method used (White et al., 2009). Similarly, in China differences of up to 30 days were reported for SOS extracted from annual SPOT NDVI time series reflective of the algorithm used (Cong et al., 2012). In addition, some RS products lack the actual acquisition date of the vegetation index, which lead to an overestimation of GSL of 5.9 days on average across the Northern Hemisphere (Wang & Zhu, 2019). The short duration of the time series, an inability to monitor individual plants and reliable determination of color change in autumn (i.e., if leaves progress through more than one color change during senescence such as green to yellow to red) present challenges when comparing with in situ

data. Even at smaller spatial scales such as at C flux tower or PhenoCam level, landscape heterogeneity within the footprint has often been cited as influencing the phenology signal thus complicating comparison with in situ observations. Satellite-derived phenology especially at coarse to medium scale resolution was found to better capture phenology when the study region had uniform species composition and topography (Melaas et al., 2016) with less agreement being observed in highly complex landscapes composed of a patchwork of small agricultural fields, urban areas, and waterbodies (Donnelly et al., 2018; Elmore et al., 2016). However, there does appear to be some instances where RS and in situ phenology were in better agreement such as at the extremes of the growing season—when buds were beginning to burst in spring and in late autumn when leaves have fallen. In addition, agreement between methods has been reported to be closer for some ecosystems than others (Browning et al., 2017; Elmore et al., 2016; Filippa et al., 2018; Peng et al., 2017; Zhang et al., 2018a).

Using colocated datasets, at a number of NEON sites in the United States, this study is the first to explore discrepancies in the timing of spring (budburst and leaf development) and autumn (leaf color and fall) phenology between in situ observations and a range of transition dates derived from MODIS and VIIRS vegetation indices and PhenoCam Green Chromatic Coordinates (GCC). Five NEON terrestrial sites were selected with differing land cover types including forest, shrubland, and grassland and for which all necessary data were available for the 3-year period 2017-2019. The specific aims of the study were to (1) determine if discrepancies between in situ- and RS-derived phenometrics varied among phenophases and/or ecosystem type, and (2) determine which (if any) RS method best captured in situ phenology. The results will demonstrate which RS technology is best suited to capture phenology across different phenophases and ecosystems and will highlight gaps in data and/or plant species collection which could be the focus of future monitoring programs at NEON sites.

# MATERIALS AND METHODS

# Study site description and climatic conditions

Five terrestrial NEON field sites (Figure 1, Table 2), of varying ecosystem type and distinct seasonality, were selected for which data for in situ phenology, PhenoCam, MODIS, and VIIRS data were available for the time period 2017–2019.

# **BOX 1** Potential reasons for discrepancies between in situ phenological observations and remote sensing (RS)-derived phenometrics

Potential cause for lack of agreement between in situ and RS phenology

### In situ observations

### General reasons

- · Monitoring usually on dominant species (usually trees) which may not represent average RS scale
- · Upscaling from individual species to community level
- · Poor spatial coverage
- Cloned plants (many networks) may not be representative of the native vegetation

# Methodological reasons

- · Differences in definitions of phenophases between networks makes comparison and interpolation difficult
- Usually limited to spring and autumn seasons
- · How to represent different phenophases from different species within the same pixel
- · Citizen science and professional network monitoring not generally in remote forested areas
- · Viewing angle different for in situ and RS—humans view from below RS (generally) from above
- · In situ observations can be subjective
- · Better agreement when observers were observing "greenness" rather than specific phenophases

# Remote sensing

## General reasons

- RS integrates topographical/landscape physical complexity
- · Land cover (vegetation) complexity: heterogeneous rural areas, rural versus urban
- · Spatial and temporal scales greater than in situ
- Short length of time series
- Better agreement at extremes of growing season and in spring in particular
- Better agreement in some ecosystems than others and in some locations than others

# Methodological reasons

- Variation occurs depending on which algorithm is used to extract SOS, EOS, etc.
- Different sensors provide different SOS dates AVHRR versus MODIS versus SPOT
- · NDVI affected by variations in solar zenith and viewing angles, and surface reflectance bidirectional effects
- · Not generally capable of monitoring individual species
- Differing sensitivities of NDVI and EVI (EVI more sensitive to chlorophyll than NDVI)
- Determining color change (if changing from green to yellow or green to yellow to red)

### Validation reasons

- · Validation of RS metrics limited to the areas and species for which in situ is available
- · Different study periods and different areas for in situ and RS
- · Different view angles—humans viewing from below, satellites from above

#### **Both**

 All methods monitoring slightly different parameters—leaf spectral properties/physiological activity/biophysical variables/direct observations ECOSPHERE 5 of 25

**TABLE 1** Summary of publications reporting comparisons between different methods of determining the timing and duration of phenophases

E		Phenometrics d	ata acquisition met	hod	Agreement			
Ecosystem type and location	Season	In situ	Satellite	Pheno Cam	C flux	— between methods	Error	Publication
One species (oak) in Harvard Forest, USA; Plot level	Spring and autumn 5 years; 2008– 2012	Ongoing monitoring; LAI; Top of canopy NDVI	MODIS NDVI and EVI	GCC (1 site)	GEP	Mixed: PC vs. Obs better in autumn; M- NDVI better vs. other methods	GCC vs. in situ RMSE 50% BB 3.6 days 95% LC 2.5 days	Keenan et al., 201
Temperate deciduous trees, rural and urban sites, Ireland; Plot level	Autumn; 1982– 2016	IPG network	AVHRR/MODIS EVI2			Poor: closer for end of season at urban site	EVI2 vs. in situ MAE 50% LC 20 days 50% LF 24 days	Donnelly et al., 201
Northern mixed forest, USA; Landscape level	Spring; 2006– 2010	High resolution, temporal and spatial observations 10 species; Research project	MODIS EVI2		GPP	Mixed: closer for very start of season	GPP vs. in situ (mean error) <10% BB: 8.6 days >90% FLO: 29.6 days EVI2 vs. in situ <10% BB 14.2 days >90% FLO 20.8 days	Donnelly et al., 2019
Northern mixed forest, USA; Landscape level	Autumn; 2010, 2012, and 2013		MODIS NDVI and EVI		GPP, NEE	Mixed: NDVI closer than other methods	NDVI vs. in situ (mean error) LC: -4 to -9 days LF: -9 to -15 days NEE vs. in situ LC: 4 to -78 days LF: -1 to -83 days	Zhau et al., 202
Deciduous broadleaf forest, evergreen needle-leaf forest; Landscape level	Spring and autumn; 2010– 2015		MODIS NDVI	GCC and NDVI (4 sites)		Mixed: good agreement for DBF; poor agreement for EF	MODIS NDVI vs. PC NDVI  RMSE spring 5 days  RMSE autumn 8 days  MODIS NDVI vs. PC GCC  RMSE spring 4 days  RMSE autumn 11 days	Filippa et al., 201
Agricultural (AG), deciduous broadleaf (DB), evergreen needle leaf (EN), grassland (GR); Landscape level	Spring and autumn; 2007– 2016 (varied with site)		NDVI MODIS	GCC (128 sites)			NDVI vs. GCC AG: SOS $5.1 \pm 27.1$ ; EOA $10.6 \pm 27.4$ DB: SOS $9.4 \pm 9.1$ ; EOA $15.0 \pm 12.9$ EN: SOS $16.6 \pm 15.3$ ; EOA $-33.4 \pm 22.7$ GR: SOS $1.4 \pm 14.5$ ; EOA $15.4 \pm 25.5$	Richardson et al., 201

# TABLE 1 (Continued)

Consistan tire		Phenometrics da	ata acquisition met	hod	Agreement between			
Ecosystem type and location	Season	In situ	Satellite	Pheno Cam	C flux	methods	Error	Publication
Contiguous	Spring and		MODIS and VIIRS	GCC and VCI			VCI vs. EVI2	Zhang
United States— deciduous	autumn; 2013– 2014		NDVI and EVI2	Vegetation Contrast Index (82			DF: SOS $5.8 \pm 5.1$ EOA $7.4 \pm 4.8$	et al., 2018
forest (DF), cropland				sites)			CR: SOS 9.4 $\pm$ 9.5 EOA 11.2 $\pm$ 7.6	
(CR), grassland (GR),							GR: SOS 9.1 $\pm$ 6.4 EOA $17.0 \pm 12.0$	
savanna (SA); Landscape level							SA: SOS 12.2 $\pm$ 9.6 EOA 29.2 $\pm$ 24.2	
outhern New Mexico,	Spring and autumn;	Citizen scientists USA-NPN	MODIS NDVI	SOS and EOS from GCC		Mixed: good for HM not for BG	In situ vs. GCC (RMSE)	Browning et al., 2017
honey mesquite C3 (HM), and	2012– 2016						BG: SOS 105.4 days; EOS 23.9 days	
black grama C4 (BG);							HM: SOS 8.6 days; EOS 16.3 days	
Plot/ landscape							NDVI vs. GCC (BG/HM)	
level							SOS 36.8 days	
							EOS 34.7 days	
United	Spring; 2000– 2013	USA-NPN;	MODIS NDVI and EVI 2000–2013		GPP 2001-2013	Mixed: DBF good, savanna weak;	NDVI/in situ 12–75 days RMSE	Peng et al., 2017
States— evergreen, deciduous,		2000–2009				EVI > NDVI	EVI/in situ 12–73 days RMSE	
and mixed forest,							NDVI/GPP 17–54 days RMSE	
shrubland, grassland, savanna, cropland, and urban; Landscape/ continental							EVI/GPP 16–53 days RMSE	
Continental United States; Landscape level	Spring; 2007	Citizen scientists USA-NPN lilac first leaf (95 sites)	MODIS EVI			Moderate	EVI vs. in situ 17.5 days RMSE	Peng et al., 2018
Southern Arizona, invasive species; Landscape level	Spring; 2011– 2013	Citizen scientists	MODIS NDVI			Moderate (based on time series)	NDVI vs. in situ 0.63 (Spearman correlation)	Wallace et al., 2016
Vestern Central Europe; Regional level	Spring; 1982– 2011	In situ PEP	AVHRR NDVI			Weak	NDVI vs. in situ 30 days earlier on average	Fu et al., 2014
North America	Spring Summer; 2004– 2013	In situ USA- NPN	MODIS MCD12Q2			Better agreement in forested pixels	Onset of greenness increase vs. NPN "Leaves" in forested pixels had an $r^2$ of 0.67	Elmore et al., 2016

(Continues)

ECOSPHERE 7 of 25

TABLE 1 (Continued)

E		Phenometrics d	ata acquisition met	hod		Agreement between		
Ecosystem type and location	Season	In situ	Satellite	Pheno Cam	C flux	methods	Error	Publication
United States and Europe; Continental level	SOS, EOS, LOS; 1999– 2017	In situ PEP and USA-NPN	SPOT- VEGETATION and PROB-V LAI, FAPAR, FCOVER, NDVI			LAI V2 closer to in situ than NDVI and others methods	LAI V2 vs. in situ (RMSE) United States: SOS 11 days; EOS 25 days Europe: SOS 9 days; EOS 28 days	Bórnez et al., 2020
Canada	SOS; 1998– 2012	In situ PlantWatch	SPOT- VEGETATION			Moderate	Greenup earlier than in situ (RMSE)  Populus tremuloides 14 days  Larix laricina 14 days  Acer rubrum 15 days  Syringa vulgaris 16 days	Delbart et al., 2015
France deciduous forest stands	SOS; 2000– 2004	In situ- project BB	MODIS NDVI MOD12Q2			Weak	RMSE 21 days Onset of greenness increase 37 days onset of greenness max	Soudani et al., 2008

Abbreviations: AVHRR, advanced very high-resolution radiometer; BB, bud burst; C flux, carbon flux; DBF, deciduous broad-leaf forest; EF, evergreen forest; EOA, end of autumn; EOS, end of season; EVI, Enhanced Vegetation Index; EVI2, Enhanced Vegetation Index-2 band; FAPAR, fraction of absorbed photosynthetically active radiation; FCOVER, fraction of green vegetation cover; FLO, full leaf open; GCC, green chromatic coordinate; GEP, gross ecosystem productivity; GPP, gross primary productivity; IPG, international phenological gardens; NEE, net ecosystem exchange; LAI-V2, Leaf Area Index (version 2); LC, leaf color; Leaves, one or more fully unfolded leaves visible on plant; LF, leaf fall; LOS, length of season; MAE, mean absolute error; M-NDVI, MODIS-Normalized Difference Vegetation Index; MODIS, moderate resolution imaging spectroradiometer; NDVI, Normalized Difference Vegetation Index; Obs, observations; PC, PhenoCam; PEP, Pan European Phenological Network; PROBA-Vegetation (European Space Agency satellite); RMSE, root mean square error; SOS, start of season; SPOT-Vegetation, Satellite Pour l'Observation de la Terre Vegetation; USA-NPN, USA-National Phenology Network; VIIRS, visible infrared imaging radiometer suite.

# In situ phenological data

The site level in situ phenological data presented in Table 3 represent pooled data of phenophase observations from two plots: the primary transect and the PhenoCam plot. The majority of the data came from primary transect observations based on 20–30 individuals of the three most abundant species within the flux tower primary air-shed.

At each NEON terrestrial site, individual plants are located along an 800-m square "loop" transect roughly comparable to a 250-m MODIS pixel (Elmendorf et al., 2016). The PhenoCam in situ phenology plot comprised a number (1–4) of individual plants within the FOV of the PhenoCam sensor. When the primary transect and the PhenoCam FOV do not overlap it is necessary to observe additional plants within the PhenoCam FOV for validation purposes. At sites with a clearly defined growing season, observations are recorded two to

three times per week during the spring and autumn seasons, whereas at sites with year-round growth, observations are recorded weekly throughout the year.

Spring and autumn phenophases observed by NEON are consistent with those defined by the USA National Phenology Network (Denny et al., 2014). Observers record "yes" when a particular phenophase is observed. Therefore, the first reported "yes" indicates the start of the phenophase and the last reported "yes" indicates the end of the phenophase. In spring, early phenophases, depending on the plant being observed, included breaking leaf buds (one or more breaking leaf buds on the plant), breaking needle buds (one or more breaking needle buds on the plant), initial growth (new growth is visible on grasses/sedges/forbs), or emerging needles (one or more emerging needles or needle bundles on the plant) and leaves (one or more fully unfolded leaves visible on the plant). The last day on which "yes"

is recorded for leaves should correspond to complete leaf fall for deciduous species. Because evergreen species do not senesce, only early season phenophase transitions are available for conifers and evergreen broadleaf species. Initial growth and leaves are observed for forbs and graminoids. Senescence phenophases observed include colored leaves (one or more leaves have turned color) and falling leaves (one or more leaves have fallen).

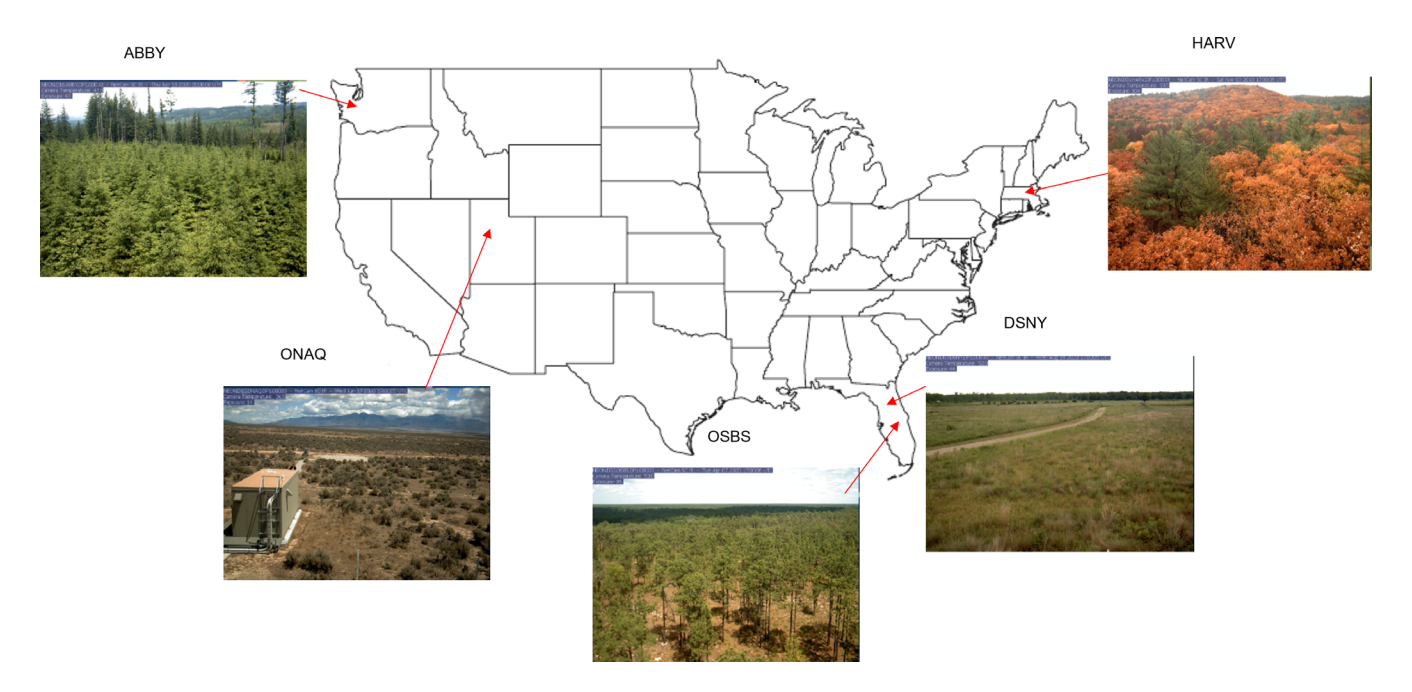


FIGURE 1 Location of the five NEON study sites with corresponding PhenoCam image representation of the vegetation type (see Table 2 for site details)

**TABLE 2** Study site characteristics (https://www.neonscience.org/field-sites/explore-field-sites)

Field site	Site ID	US state; Lat./long.	Eco-climatic domain	Dominant NLCD class	Elevation and climate <sup>a</sup>	Relevant data
Harvard Forest	HARV	MA; 42.5369;	Northeast	Deciduous forest; evergreen	348 m, 7°C,	in situ
	D01	-72.17266		forest; mixed forest; woody wetlands	1199 mm	08/14
				wettarids		PhenoCam
						C Flux
Onaqui	ONAQ D15	UT; 40.17759; -112.45244	Great Basin	Evergreen forest; shrub/scrub	1662 m, 9°C, 288 mm	in situ 07/14
						PhenoCam
						C Flux
Ordway-Swisher	OSBS	FL; 29.68927;	Southeast	Emergent herbaceous wetlands;	46 m, 21°C,	in situ
Biological	D03	-81.99343		evergreen forest; woody	1302 mm	PhenoCam
Station				wetlands		C Flux
Disney Wilderness	DSNY	FL; 28.12504;	Southeast	Pasture/hay; woody wetlands	20 m, 23°C,	in situ
Preserve	D03	-81.4362			1216 mm	PhenoCam
						C Flux
Abby Road	ABBY	WA; 45.76243;	Pacific	Evergreen forest; grassland/	365 m, 10°C,	in situ
	D16	-122.33033	Northwest	herbaceous shrub/scrub	2451 mm	PhenoCam
						C Flux

Abbreviation: NLDC, National Land Cover Database class.

<sup>&</sup>lt;sup>a</sup>Values are given for elevation, temperature, and annual average precipitation, respectively.

ECOSPHERE 9 of 25

# PhenoCam: green chromatic coordinate

Data for the study sites were extracted from the PhenoCam Dataset V2.0 (Milliman et al., 2019; Seyednasrollah et al., 2019a, 2019b, 2019c) whereby digital images were collected at 15-min intervals over a 24-h period. Canopy greenness time-series data were obtained from these images by delineating appropriate regions of interest (ROIs) and calculating the green chromatic coordinate (GCC) for each, using the following equation:

$$GCC = G_{DN}/(R_{DN} + G_{DN} + B_{DN}),$$

where  $R_{\rm DN}$ ,  $G_{\rm DN}$ , and  $B_{\rm DN}$  are the average red, green, and blue digital values, respectively, within the ROIs. After extracting GCC values, time series were obtained from the 90th percentile of canopy greenness at 3-day intervals. Phenological transition dates corresponding to the start of each "greenness rising" and the end of each

"greenness falling" were calculated from the summary time-series products (i.e., 1-day and 3-day time series) using locally weighted scatterplot smoothing (LOESS). GCC T10, T25, and T50 are GCC transition dates corresponding to 10th, 25th, and 50th percentiles, respectively, from the GCC\_90 smoothing line. Further details on the PhenoCam dataset and image processing are discussed in Seyednasrollah et al., 2019a, 2019b.

# Satellite data: MODIS and VIIRS vegetation indices

The MODIS Collection 6, 500 m daily Nadir BRDF-Adjusted Reflectance product (MOD09GQ/MYD09GQ) and BRDF-Albedo Quality product (MOD09GQ/MYD09GQ) were used to calculate the EVI2 and NDVI time series. Both MODIS products were retrieved for the  $2 \times 2$  pixels closest to each NEON site location using Google Earth Engine.

**TABLE 3** Metadata for in situ phenology data at each of five terrestrial sites in the United States' NEON (Harvard Forest [MA], Onaqui [UT], Abby Road [WA], Disney Wilderness Preserve [FL], and Ordway-Swisher Biological Station [FL]), including list of species and growth form

Species name by site	<b>Growth form</b>	2017	2018	2019
HARV				
Acer rubrum L (N)	DB	54	42	42
Aralia nudicaulis L. (N) wild sarsaparilla	Forb	53	42	41
Quercus rubra L. (N)	DB	57	44	43
ONAQ				
Artemisia tridentata Nutt. (N) big sagebrush	Drought DB	41	41	36
Bromus tectorum L. (NN) Cheatgrass	Gram.	34	41	36
Ceratocephala testiculata (Crantz) Roth (I) bur buttercup	Forb	28	41	22
OSBS				
Aristida beyrichiana Trin. & Rupr. (N)	Gram.	43	49	15
Pinus palustris Mill. (N)	Pine: EC	43	49	15
Quercus laevis Walter (N)	DB	43	49	15
DSNY				
Andropogon virginicus L. (N)	Gram.	41	48	22
Aristida beyrichiana Trin. & Rupr. (N)	Gram.	41	48	22
Euthamia caroliniana (L.) Greene ex Porter & Britton (N)	Forb	41	48	22
ABBY				
Corylus cornuta Marshall var. californica (A. DC.) Sharp (N)	DB	53	52	54
Gaultheria shallon Pursh (N)	EB	45	42	45
Pseudotsuga menziesii (Mirb.) Franco var. menziesii (N)	EC	52	53	54

Daily NDVI/EVI2 values were aggregated to 3-day composites by selecting the maximum EVI2 value with the best quality and the corresponding NDVI within a 3-day period, which would reduce the uncertainties and improve the processing speed while retaining the fine temporal resolution of the EVI2 time series. Then, unusually large EVI2 values, caused by inaccurate atmospheric correction or other factors, were identified as those larger than 90% of the corresponding NDVI values, and removed (Zhang et al., 2018b). Further, EVI2 time series were smoothed using a Savitzky-Golay filter and a running local median filter. Finally, the widely used piecewise logistic functions (Zhang et al., 2003) were applied to EVI2 to retrieve the phenological transition dates across site-years. Similarly, the VIIRS, 500 m daily Nadir BRDF-Adjusted Reflectance product (VNP43IA4) was used to calculate EVI2 and NDVI time series for the  $2 \times 2$  pixels around each NEON site. In

addition, the VIIRS land surface phenology product (VNP22Q2) was used to directly retrieve phenological transition dates (Zhang et al., 2020). The median over four pixels of all satellite-based time series and phenological transition dates were used in all statistical analyses.

# Phenesse estimates of in situ phenological transition dates

For each site-year-species-phenophase combination with at least 25 observation counts, we estimated the 1st, 5th, 50th, 95th, and 99th percentiles of spring and autumn phenophases using a newly developed R package, phenesse v0.1.1 (Belitz et al., 2020). Each day of year with a "yes" observation for a particular phenophase per site-year-species combination was included in the list of observations used to

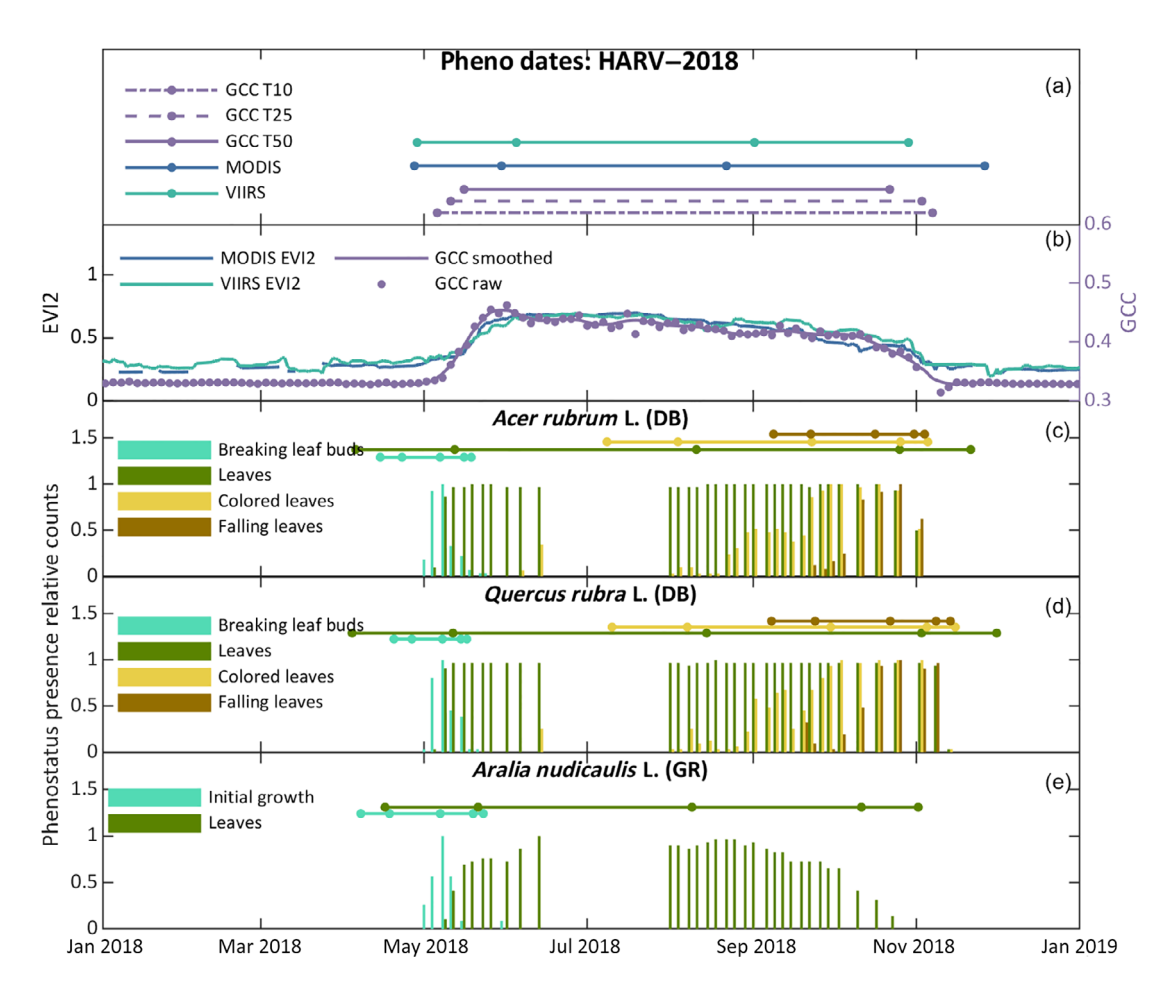


FIGURE 2 Suite of phenometrics extracted for the Harvard Forest, MA (HARV) NEON site for 2018. (a) Phenological transition dates (dots) based on PhenoCam GCC, MODIS-EVI2, and VIIRS-EVI2. GCC T10, T25, and T50 represent transition dates corresponding to the 10th, 25th, and 50th percentiles for greenness rising in spring and greenness falling in autumn based on the GCC 90th percentile smoothed line. (b) Time series of MODIS EVI2 (daily and 500-m resolutions), VIIRS EVI2 (daily and 500-m resolutions), PhenoCam GCC raw data and smoothed line. (c)–(e) In situ phenological presence observations (bars) for breaking leaf buds, leaves, colored leaves, and falling leaves of deciduous broadleaf, or initial growth and leaves for grass, and phenesse estimated phenological transition dates (dots). From left to right, for in situ phenesse estimates, dots are dates corresponding to 1st, 5th, 50th, 95th, and 99th percentiles, respectively. Figures for 2017 and 2019 are available in Appendix S1: Figure S1a,b

ECOSPHERE 11 of 25

generate the phenological estimates. Phenology estimates were generated using the weib\_percentile() function from the R package phenesse, in which the in situ phenology observations were used to generate Weibull-parameterized estimates for any percentile of a distribution. This approach has been demonstrated to generate accurate and unbiased phenological estimates if the underlying phenophase follows a unimodal distribution (Belitz et al., 2020). We used estimates of the 5th, 50th, and 95th percentiles as proxies for the start, middle, and end of each phenophase, respectively.

# Integrated plot comparison of in situ and RS phenology

In order to evaluate relationships between in situ and remotely sensed phenometrics, we examined all species at each site and selected only those exhibiting a distinct seasonality profile for which to compare with RS metrics. All species at ABBY and HARV were retained for both spring and autumn comparisons (Figures 2–6). Only spring phenophases were available for the grassland species at DSNY, and since "leaves" were present all year-round (Figure 5), "initial growth" was the only phenophase included in the scatterplots. Similarly, at OSBS, only breaking leaf bud (*Quercus laevis*) and emerging needles (*Pinus palustris*) were included because leaves, colored leaves, and leaf fall were recorded year-round for *Q. laevis* and, initial growth and leaves were also recorded year-round for *Aristida beyrichiana* (Figure 4). Finally, at ONAQ, *Artemisia tridentata* data were omitted as all phenophases were recorded year-round (Figure 3).

Two sites, ABBY (Corylus cornuta) and HARV (Quercus rubra; Acer rubrum), had sufficient estimated in

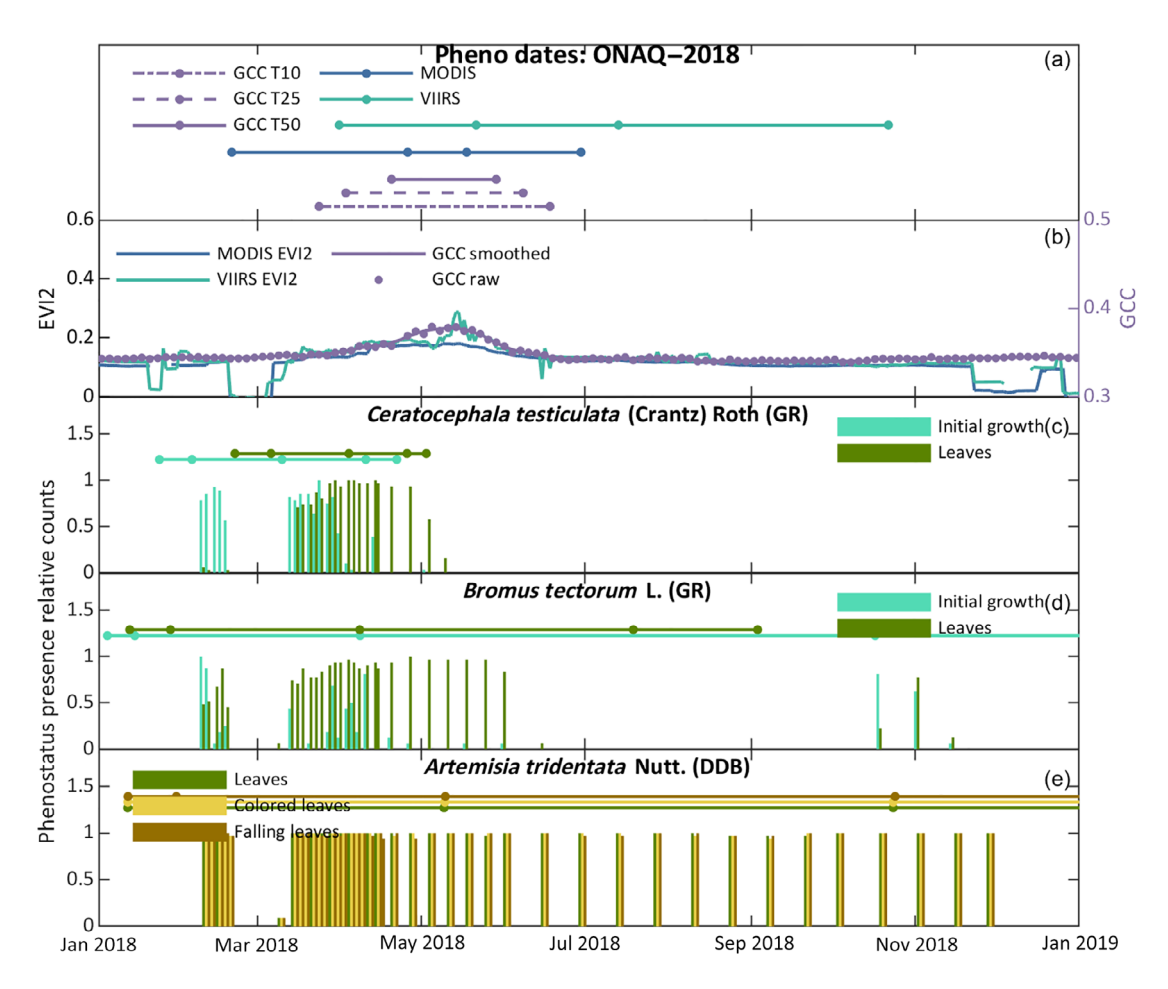


**FIGURE 3** Suite of phenometrics extracted for the Onaqui, UT (ONAQ), NEON site for 2018. (a) Phenological transition dates (dots) based on PhenoCam GCC, MODIS-EVI2, and VIIRS-EVI2. GCC T10, T25, and T50 represent transition dates corresponding to the 10th, 25th, and 50th percentiles for greenness rising in spring and greenness falling in autumn based on the GCC 90th percentile smoothed line. (b) Time series of MODIS EVI2 (daily and 500-m resolutions), VIIRS EVI2 (daily and 500-m resolutions), PhenoCam GCC raw data and smoothed line. (c)–(e) In situ phenological presence observations (bars) for breaking leaf buds, leaves, colored leaves, and falling leaves of deciduous broadleaf, or initial growth and leaves for grass, and phenesse estimated phenological transition dates (dots). From left to right, for in situ phenesse estimates, dots are dates corresponding to 1st, 5th, 50th, 95th, and 99th percentiles, respectively. Figures for 2017 and 2019 available in Appendix S1: Figure S2a,b

situ autumn (leaf color and leaf fall) data to use for comparison with remotely sensed phenometrics. Autumn phenophases were not observed at DSNY and species for which leaf color and leaf fall data were recorded at ONAQ (*A. tridentata*) and OSBS (*Q. laevis*) spanned the entire year and therefore not specific to autumn.

# Statistical analysis

Linear regression was used to test the significance of the relationship between in situ phenological estimates and all remotely sensed phenometrics for both spring and autumn seasons. In addition, both root mean square error (RMSE) and mean bias error (MBE) were calculated to measure the magnitude of the error and overall bias between in situ and RS phenometrics.

Pearson correlation coefficients were computed between PhenoCam GCC (90th percentile) and different lags (0–180 days) of NDVI, EVI2 derived from MODIS, and VIIRS to examine the existence of lag effects that is, whether or not satellite and PhenoCam sensors viewed similar phenological phenomena from space and near surfaces. Lag correlations were calculated as follows:

$$r_k = \frac{\sum_{t=t_1}^{n-k} \left( \text{GCC}_t - \overline{\text{GCC}} \right) \left( \text{VI}_{t+k} - \overline{\text{VI}} \right)}{\sqrt{\sum_{t=t_1}^{n-k} \left( \text{GCC}_t - \overline{\text{GCC}} \right)^2} \sqrt{\sum_{t=t_1}^{n-k} \left( \text{VI}_t - \overline{\text{VI}} \right)^2}},$$

 $VI \in \{MODIS_{NDVI}, VIIRS_{NDVI}, MODIS_{EVI2}, MODIS_{EVI2}\},$ 

where  $GCC_t$  is the GCC value on a specific date (e.g., 7 May 2019),  $VI_{t+k}$  is the vegetation index value at k days lag of  $GCC_t$  (e.g.,  $VI_{t+k}$  at 5 days lag, 12 May 2019). For instance,

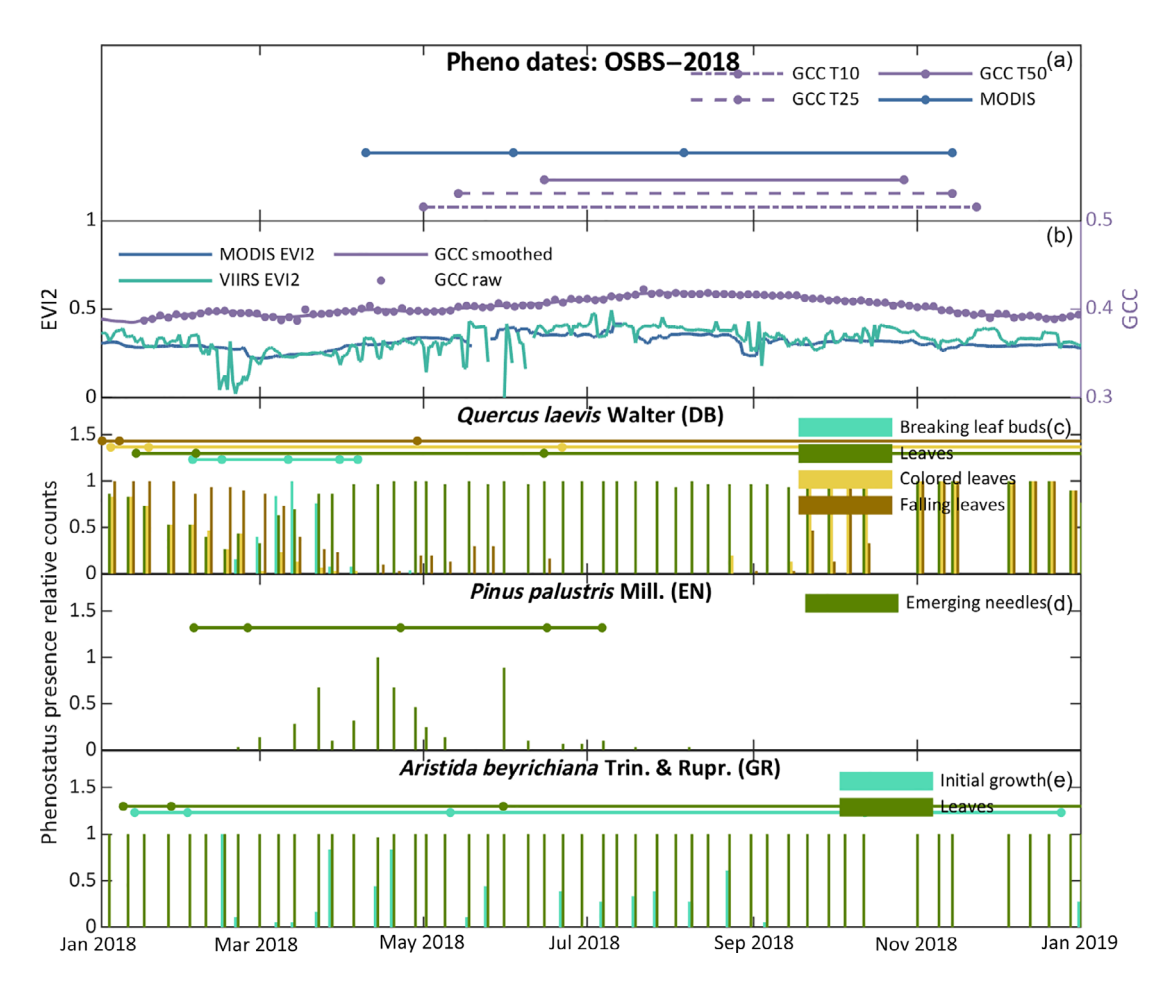


**FIGURE 4** Suite of phenometrics extracted for the Ordway-Swisher Biological Station, FL (OSBS), NEON site for 2018. (a) Phenological transition dates (dots) based on PhenoCam GCC, MODIS-EVI2, and VIIRS-EVI2. GCC T10, T25, and T50 represent transition dates corresponding to the 10th, 25th, and 50th percentiles for greenness rising in spring and greenness falling in autumn based on the GCC 90th percentile smoothed line. (b) Time series of MODIS EVI2 (daily and 500-m resolutions), VIIRS EVI2 (daily and 500-m resolutions), PhenoCam GCC raw data and smoothed line. (c)–(e) In situ phenological presence observations (bars) for breaking leaf buds, leaves, colored leaves, and falling leaves of deciduous broadleaf, or initial growth and leaves for grass, and phenesse estimated phenological transition dates (dots). From left to right, for in situ phenesse estimates, dots are dates corresponding to 1st, 5th, 50th, 95th, and 99th percentiles, respectively. Figures for 2017 and 2019 available in Appendix S1: Figure S3a,b

ECOSPHERE 13 of 25

if  $GCC_t$  is the current observation, then  $VI_{t+k}$  is the VI value at k days after the current date.  $t_1$  does not have a specific range. It differs with respect to site and satellite product.  $t_1$ s for HARV (MODIS: 13 September 2016, VIIRS: 13 September 2016), DSNY (MODIS: 16 September 2016, VIIRS: 16 September 2016), OSBS (MODIS: 16 September 2016, VIIRS: 16 September 2016), ONAQ (MODIS: 19 September 2016, VIIRS: 19 September 2016), ABBY (MODIS: 24 March 2017, VIIRS: 13 April 2017). n also differs with respective to site and satellite product. ns for HARV (MODIS: 4 July 2019, VIIRS: 16 June 2019), DSNY (MODIS: 4 July 2019, VIIRS: 4 July 2019), OSBS (MODIS: 4 July 2019, VIIRS: 4 July 2019), ONAQ (MODIS: 30 May 2019, VIIRS: 16 June 2019), ABBY (MODIS: 13 June 2019, VIIRS: 3 June 2019), GCC is the mean of GCC from time  $t_1$  to time n-k, while  $\overline{\text{VI}}$  represents the mean of VI from  $t_1 + k$  to n, respectively.

# RESULTS

# RS and in situ phenometrics extracted from NEON sites

All phenometrics (phenesse estimates [in situ], MODIS-EVI2, VIIRS-EVI2, and PhenoCam GCC) for each year at each site were plotted for comparison of annual phenological dynamics. Only figures for 2018 are presented representing the annual phenological profiles for each phenometric (Figures 2–6). Similar figures for 2017 and 2019 are available in Appendix S1: Figures S1–S5. The range of habitats and species present at each site was reflected in large intersite variation in phenology (Figures 2–6). Across all sites, GSL derived from MODIS-EVI2 and VIIRS-EVI2 transition dates was consistently longer than similar metrics derived from GCC (Figures 2a–6a).

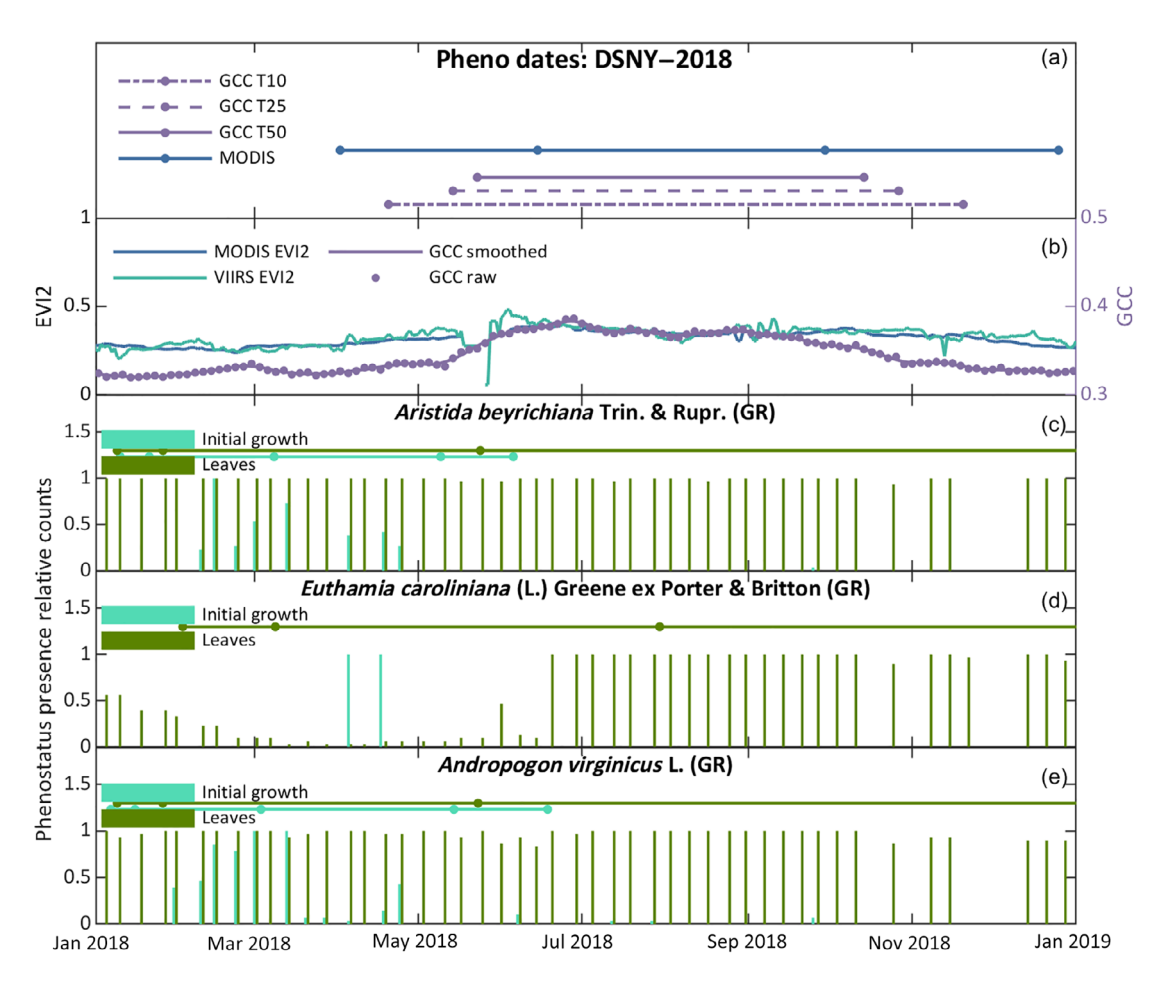


FIGURE 5 Suite of phenometrics extracted for the Disney Wilderness Preserve, FL (DSNY), NEON site for 2018. (a) Phenological transition dates (dots) based on PhenoCam GCC, MODIS-EVI2, and VIIRS-EVI2. GCC T10, T25, and T50 represent transition dates corresponding to the 10th, 25th, and 50th percentiles for greenness rising in spring and greenness falling in autumn based on the GCC 90th percentile smoothed line. (b) Time series of MODIS EVI2 (daily and 500-m resolutions), VIIRS EVI2 (daily and 500-m resolutions), PhenoCam GCC raw data and smoothed line. (c)–(e) In situ phenological presence observations (bars) for breaking leaf buds, leaves, colored leaves, and falling leaves of deciduous broadleaf, or initial growth and leaves for grass, and phenesse estimated phenological transition dates (dots). From left to right, for in situ phenesse estimates, dots are dates corresponding to 1st, 5th, 50th, 95th, and 99th percentiles, respectively. Figures for 2017 and 2019 available in Appendix S1: Figure S4a,b

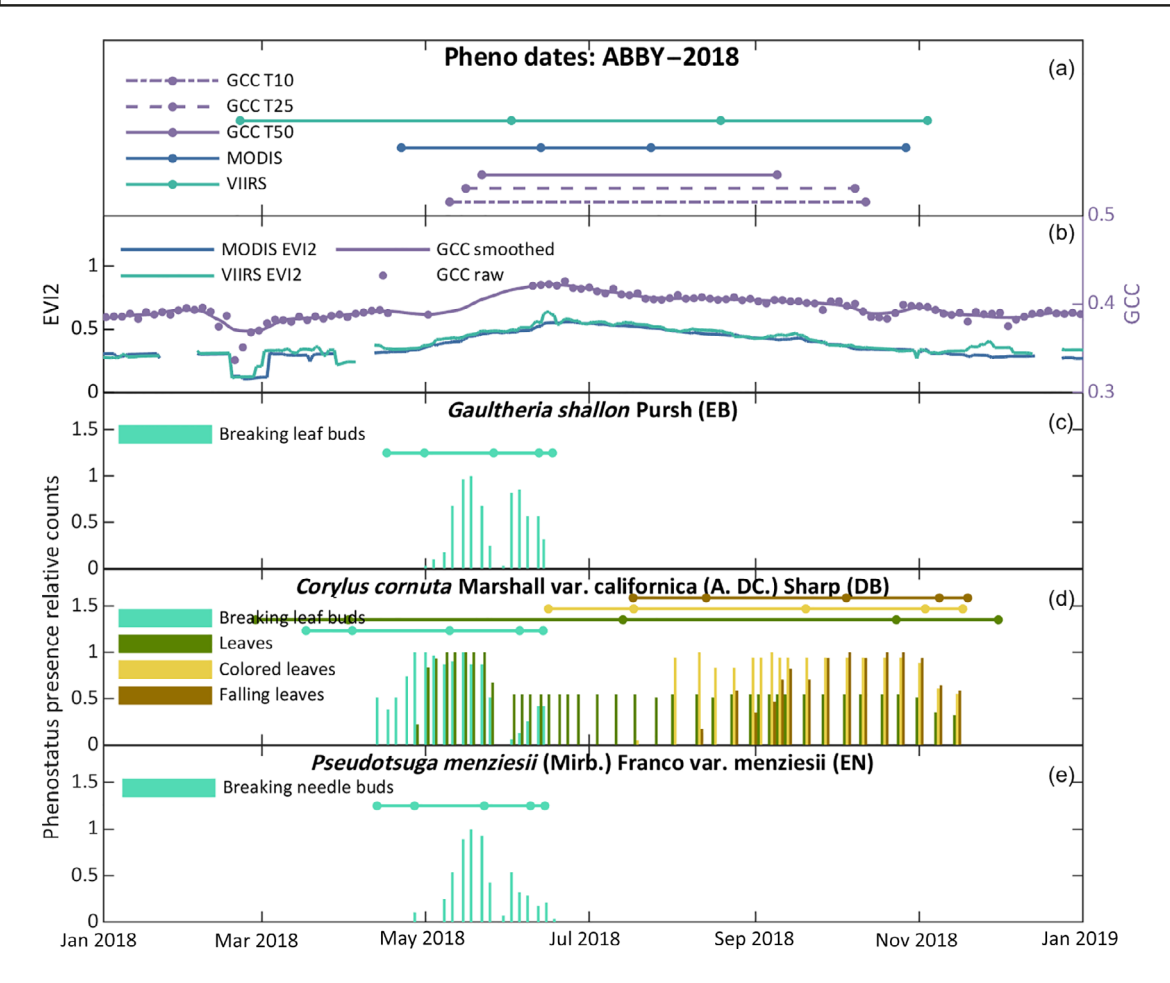


FIGURE 6 Suite of phenometrics extracted for the Abby Road, WA (ABBY), NEON site for 2018. (a) Phenological transition dates (dots) based on PhenoCam GCC, MODIS-EVI2, and VIIRS-EVI2. GCC T10, T25, and T50 represent transition dates corresponding to the 10th, 25th, and 50th percentiles for greenness rising in spring and greenness falling in autumn based on the GCC 90th percentile smoothed line. (b) Time series of MODIS EVI2 (daily and 500-m resolutions), VIIRS EVI2 (daily and 500-m resolutions), PhenoCam GCC raw data and smoothed line. (c)–(e) In situ phenological presence observations (bars) for breaking leaf buds, leaves, colored leaves, and falling leaves of deciduous broadleaf, or initial growth and leaves for grass, and phenesse estimated phenological transition dates (dots). From left to right, for in situ phenesse estimates, dots are dates corresponding to 1st, 5th, 50th, 95th, and 99th percentiles, respectively. Figures for 2017 and 2019 available in Appendix S1: Figure S5a,b

**TABLE 4** Regression relationships between phenesse estimates of in situ phenology and MODIS-EVI2-derived spring phenometrics across all species, sites, and years

	MODIS green-up			MODIS	MODIS mid-green			MODIS maturity		
In situ phenesse estimates	p	Slope	R <sup>2</sup>	p	Slope	R <sup>2</sup>	p	Slope	R <sup>2</sup>	
Early phenophases										
$P_5$	0.000	0.935	0.291	0.000	0.903	0.203	0.032	0.503	0.073	
P <sub>50</sub>	0.000	0.625	0.190	0.003	0.610	0.135	0.054	0.375	0.060	
Leaves										
P <sub>5</sub>	0.000	1.019	0.634	0.000	1.308	0.662	0.000	1.412	0.574	
P <sub>50</sub>	0.000	1.701	0.858	0.000	2.183	0.896	0.000	2.338	0.765	

*Notes*: Early phenophases include breaking leaf bud, breaking needle bud, emerging needles, and initial growth. Leaves indicate one or more unfolded leaves present.  $P_5$ ,  $P_{50}$ , and  $P_{95}$  refer to the dates corresponding to the 5th, 50th, and 95th percentiles of phenesse estimates, respectively. The p values in boldface are significant at the 0.05 level.

ECOSPHERE 15 of 25

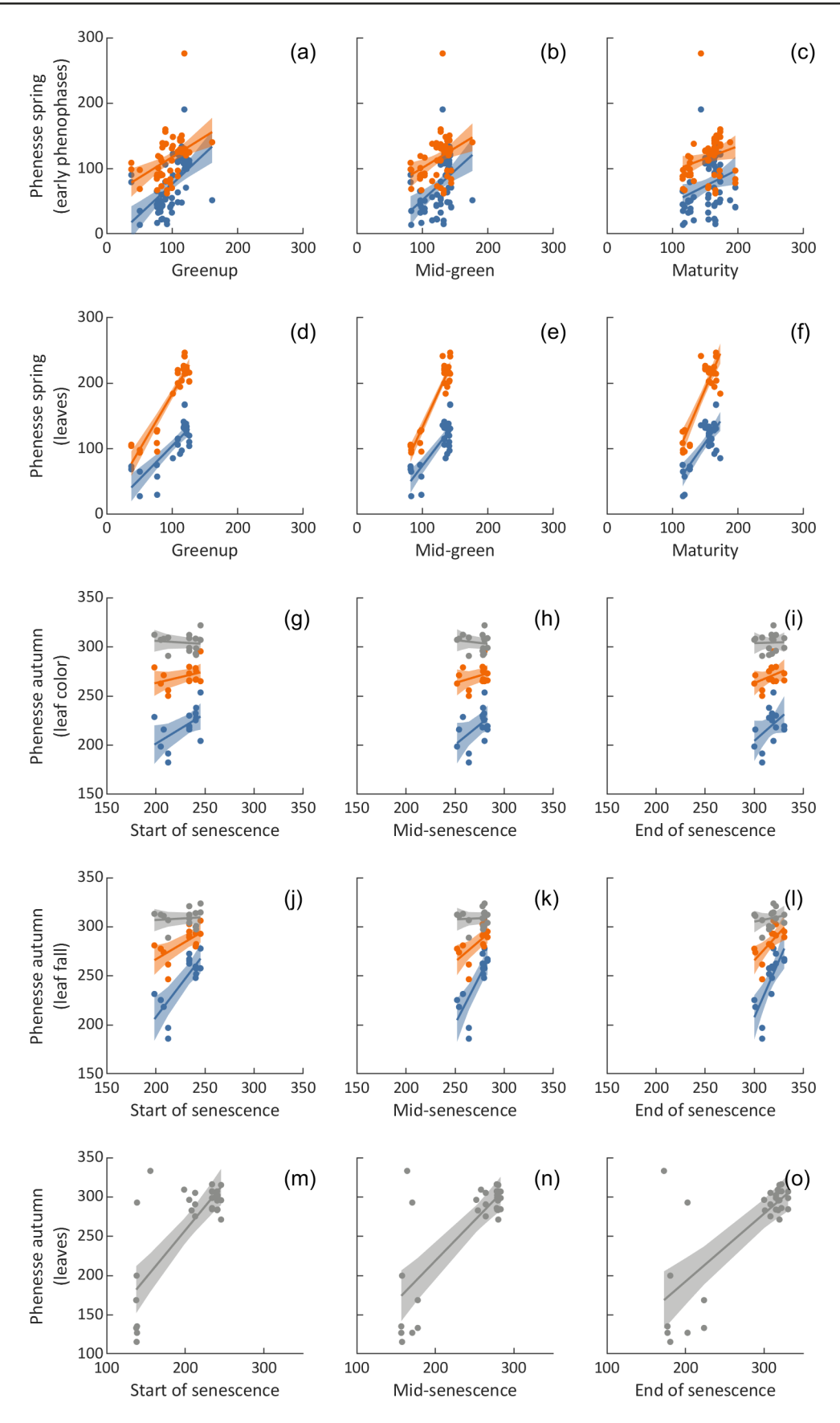


FIGURE 7 Legend on next page.

**TABLE 5** Root mean square error (RMSE) and mean bias error (MBE) values in days between phenesse estimates (Est\_05, 5th percentile date; Est\_50, 50th percentile date) of in situ early spring phenophases and MODIS-EVI2, VIIRS-EVI2, and PhenoCam-GCC (GCC T10, T25, and T50 representing 10th, 25th, and 50th percentiles of greenness rising)-derived phenometrics

		MODIS—spring		VIIRS-	-spring		GCC			
Error estimate	Phenesse estimate	GU	Mid-G	Mat	GU	Mid-G	Mat	T10	T25	T50
RMSE	Est_05	39.9***	61.0***	87.4**	45.1	49.6	64.3**	59.1**	69.2	83.3
	Est_50	35.2***	31.9**	50.0*	70.3	64.6	67.4	24.8***	33.2	45.3
MBE	Est_05	23.1***	50.3***	78.4**	3.6	29.7	57.7**	48.9**	58.6	72.1
	Est_50	-18.4***	8.8**	37.0*	-24.4	1.6	29.6	10.5***	20.2*	33.7

Notes: Bold text indicates statistically significant regression relationships at p < 0.05; p < 0.01; p < 0.001. Abbreviations: GU, Greenup; Mid-G, mid-green; Mat, maturity.

In 2018, VIIRS-GSL tended to be shorter than MODIS-GSL for the site dominated by deciduous forest (HARV), and longer at both the grassland and evergreen forest sites (ONAQ and ABBY) (Figures 2a, 3a, and 6a). This relationship was not consistent across all years and sites (Appendix S1: Figures S1a,b, S2a,b, and S5a,b). The MODIS and VIIRS time series (Figures 2b, 3b, and 6b) showed similar trends at each site apart from OSBS in which VIIRS was more variable than MODIS (Figure 4b). In comparison to the satellite-derived EVI2 time series' GCC exhibited a slightly more defined growing season, at each site, reflective of the higher resolution. Sites at which evergreen vegetation was present (OSBS and ABBY) showed higher and more consistent GCC values throughout the year than sites with deciduous species and/or herbaceous species (Figures 2b-6b). Phenesse estimates effectively captured spring and autumn phenophases especially for deciduous species with clear start and end dates (Figures 2c-e to 6c-e). However, for species such as A. tridentata at ONAQ (Figure 3e) that exhibited continuous development throughout the year phenesse estimates were less meaningful. The species level in situ data exhibited annual phenological profiles typical of their site-specific ecosystem. Broadleaf deciduous tree and shrub species, maple (A. rubrum), oak (Q. rubra), and hazel (C. cornuta) (HARV: Figure 2c,d; ABBY: Figure 6d) showed well-defined start and end dates in spring and autumn characteristic of deciduous and mixed forest habitats. The herbaceous species (Ceratocephala testiculata, Bromus tectorum) at ONAQ in the Great Basin exhibited a short growing season concentrated in spring whereas the drought-deciduous shrub (A. tridentata) showed development during most of the year typical of cool dry conditions (Figure 3). In situ phenological profiles exhibited continuous presence of leaves year-round at OSBS and DSNY for the herbaceous species (A. beyrichiana, Euthamia caroliniana, Andropogon virginicus) and the deciduous broadleaf (Q. laevis), which is reflective of warm wetland conditions (Figures 4e and 5c-e). Finally, only spring phenophases were available for the evergreen species (P. palustris, Gaultheria shallon, Pseudotsuga menziesii) at OSBS and ABBY and were characteristic of initial emergence in the spring season (Figures 4d and 6c,e).

# Regression results between in situ phenological dates estimates and RS phenometrics across NEON sites

The timing (the last day of the year [DOY]) (across species, sites, and years) of in situ phenophase estimates (5th and

**FIGURE 7** Scatterplots comparing phenesse estimates (DOY) of in situ phenology with a suite of MODIS-EVI2-derived phenometrics (DOY) across all species, sites, and years. Phenesse  $P_5$  (blue dots),  $P_{50}$  (orange dots), and  $P_{95}$  (gray dots) represent the 5th, 50th, and 95th percentile dates, respectively. (a) Phenesse spring (breaking leaf bud, breaking needle bud, emerging needles, initial growth; HARV, ONAQ, OSBS, DSNY, ABBY) estimates versus MODIS Greenup; (b) phenesse spring estimates versus MODIS mid-green; (c) phenesse spring estimates versus MODIS mid-green; (d) phenesse leaves estimates versus MODIS maturity; (g) phenesse leaves estimates versus MODIS start of senescence; (h) phenesse leaf color estimates versus MODIS mid-senescence; (i) phenesse leaf color estimates versus MODIS end-senescence; (j) phenesse leaf fall (HARV, ABBY) estimates versus MODIS mid-senescence; (k) phenesse leaf fall estimates versus MODIS mid-senescence; (h) phenesse leaf fall estimates versus MODIS mid-senescence; (n) phenesse leaf self fall estimates versus MODIS start of senescence; (n) phenesse leaf self self self self self self self-senescence; (n) phenesse leaves estimates versus MODIS mid-senescence; (o) phenesse leaves estimates versus MODIS end-senescence; (n) phenesse leaves estimates versus MODIS mid-senescence; (n) phenesse leaves versus MODIS mid-senescence; (n) phenesse leaves estimates versus MODIS mid-senescence; (n) phenesse leaves versus MODIS end-senescence; (n) phenesse leaves versus MODIS mid-senescence; (n) phenesse leaves versus MODIS end-senescence; (n) phenesse leaves versus MODIS mid-senescence; (n) phenesse leaves versus MODIS end-senescence; (n) phenesse leaves versus MODIS mid-senescence; (n) phenesse leaves versus MODIS end-senescence; (n) phenesse leaves versus MODIS mid-senescence; (n) phenesse leaves versus MODIS end-senescence; (n) phenesse

ECOSPHERE 17 of 25

50th percentile dates) of early spring were significantly (p values varied between 0.000 and 0.054) correlated with MODIS greenup, mid-green, and maturity dates (Table 4, Figure 7). RMSE and MBE values were consistently lower for the 50th percentile phenesse dates (RMSE: 31.9-50.0 days; MBE: -18.4 to 37 days) than for the 5th percentile dates (RMSE: 39.9-87.4 days; MBE: 23.1-78.4 days) (Table 5). Similarly, the average timing of leaves (5th and 50th percentile dates) was significantly (p = 0.000) correlated with MODIS greenup, mid-green, and maturity. RMSE (21.7 days) and MBE (-4.6 days) values were lower between leaves (5th percentile) and MODIS greenup than for any other spring in situ estimates and MODIS phenometrics (Table 6). Surprisingly, there was only one significant correlation between the timing of in situ estimates of autumn leaf color (5th percentile dates) and MODIS phenometrics (start of senescence) although the timing of leaf fall (5th and 50th percentile dates) was significantly correlated with the start (RMSE: 24.5 days; MBE: –16.9 days), mid (RMSE: 33.7 days; MBE: 27.3 days), and end (RMSE: 74.0 days; MBE: 70.9 days) of senescence (Tables 7–10, Figure 7). In addition, later season in situ leaves estimates (95th percentile dates) were significantly correlated with MODIS-derived start, mid, and end of senescence but with high RMSE (47.3–72.8 days) and MBE (–58.4 to 18.3 days) values (Tables 7 and 8, Figure 7).

The in situ estimated dates of early (5th percentile) phenophases showed a statistically significant (p=0.005) relationship with VIIRS maturity dates (Table 11), but with relatively high RMSE (64.3 days) and MBE (57.7 days) values (Table 5). The timing of early in situ phenesse estimates (5th and 50th percentile dates) of

**TABLE 6** Root mean square error (RMSE) and mean bias error (MBE) values between phenesse estimates (Est\_05, 5th percentile date; Est\_50, 50th percentile date) of in situ "leaves" phenophases and MODIS-EVI2, VIIRS-EVI2, and PhenoCam-GCC (GCC T50, T25, and T10 representing 50th, 25th, and 10th percentiles of greenness falling)-derived phenometrics

Error	Phenesse	MODIS—	MODIS—leaves			leaves		GCC			
estimate	estimate	GU	Mid-G	Mat	GU	Mid-G	Mat	T10	T25	T50	
RMSE	Est_05	21.7***	28.1***	47.9***	28.4**	37.2***	57.9***	24.1****	30.8***	40.0**	
	Est_50	89.4***	69.5**	52.6***	92.7**	72.5**	56.8***	72.9****	68.1***	63.2**	
MBE	Est_05	<b>-4.6***</b>	18.2***	41.4***	-1.2**	23.4***	48.5***	11.9***	19.4***	28.8**	
	Est_50	-85.3***	-62.5**	-39.3***	-81.9**	-57.3**	-32.2***	<b>-66.0***</b>	-58.5***	<b>-49.1***</b>	

Notes: Spring-derived GCC transition dates run from T10 to T50 reflecting "greenness rising." Bold text indicates statistically significant regression relationships at \*p < 0.05; \*\*p < 0.01; \*\*\*p < 0.001.

Abbreviations: GU, greenup; Mid-G, mid-green; Mat, maturity.

**TABLE 7** Regression relationships between phenesse estimates of in situ phenology and MODIS-EVI2-derived autumn phenometrics across all species, sites, and years

	MODIS start senescence			MODIS	mid-senesce	ence	MODIS end-senescence		
In situ phenesse estimates	p	Slope	R <sup>2</sup>	p	Slope	R <sup>2</sup>	p	Slope	$R^2$
Leaf color									
$P_5$	0.041	0.608	0.283	0.071	0.811	0.229	0.111	0.883	0.184
P <sub>50</sub>	0.197	0.238	0.125	0.278	0.299	0.090	0.205	0.420	0.120
P <sub>95</sub>	0.689	-0.064	0.013	0.611	-0.117	0.021	0.917	0.029	0.0071
Leaf fall									
$P_5$	0.001	1.310	0.593	0.001	1.946	0.596	0.001	2.292	0.560
P <sub>50</sub>	0.012	0.592	0.394	0.016	0.852	0.372	0.010	1.094	0.415
P <sub>95</sub>	0.718	0.058	0.010	0.853	0.042	0.003	0.477	0.202	0.040
Leaves									
P <sub>95</sub>	0.000	1.208	0.601	0.000	1.027	0.597	0.000	0.863	0.554

Notes: Leaves indicates one or more unfolded leaves present.  $P_5$ ,  $P_{50}$ , and  $P_{95}$  refer to the dates corresponding to the 5th, 50th, and 95th percentiles of phenesse estimates, respectively. The p values in boldface are significant at the 0.05 level.

**TABLE 8** RMSE (root mean square error) and MBE (mean bias error) values between phenesse estimates (Est\_95, 95th percentile date, senescence) of in situ "leaves" phenophases and MODIS-EVI2, VIIRS-EVI2, and PhenoCam-GCC (GCC T50, T25, and T10 representing 50th, 25th, and 10th percentiles of greenness falling)-derived phenometrics

Error	Phenesse	MODIS—	leaves	VIIRS—le	eaves		GCC			
estimate	estimate	Start	Mid	End	Start	Mid	End	T50	T25	T10
RMSE	Est_95	72.8***	47.3***	49.2***	66.3***	59.9***	73.8***	41.6***	37.1***	37.1***
MBE	Est_95	-58.4***	-20.2***	18.3***	-31.4***	5.2***	40.8***	-14.4***	-1.9***	2.8***

Notes: Bold text indicates statistically significant regression relationships at \*p < 0.05; \*\*p < 0.01; \*\*\*p < 0.001.

**TABLE 9** Root mean square error (RMSE) and mean bias error (MBE) values in days between phenesse estimates (Est\_05, 5th percentile date; Est\_50, 50th percentile date; Est\_95, 95th percentile date) of in situ early autumn phenophases (leaf color) and MODIS-EVI2, VIIRS-EVI2, and PhenoCam-GCC (GCC T50, T25, and T10 representing 50th, 25th, and 10th percentiles of greenness falling)-derived phenometrics

		MODIS—leaf color			VIIRS-	-leaf color				
		Senescence		Senescence			GCC—leaf color			
Error estimate	Phenesse estimate	Start	Mid	End	Start	Mid	End	T50	T25	T10
RMSE	Est_05	19.0*	56.2	98.9	28.7	56.7	89.7	70.1	85.1	89.4
	Est_50	43.4	12.8	47.6	37.8	14.0	38.5	27.5	32.5	36.1
	Est_95	78.1	34.8	17.0	69.8	34.8	110.8	35.4	15.7	12.4
MBE	Est_05	9.6*	53.9	97.5	17.7	53.1	87.5	64.9	82.3	87.0
	Est_50	-41.6	2.7	46.3	-33.5	1.9	36.3	11.4	38.8	33.5
	Est_95	-75.9	-31.6	12.0	-67.8	-32.4	2.0	-24.9	-7.5	-2.8

Notes: No statistically significant relationships were recorded. Bold text indicates statistically significant regression relationships at \*p < 0.05; \*\*p < 0.01; \*\*\*p < 0.001.

**TABLE 10** RMSE (root mean square error) and MBE (mean bias error) values in days between phenesse estimates (Est\_05, 5th percentile date; Est\_50, 50th percentile date; Est\_95, 95th percentile date) of in situ early autumn phenophases (leaf fall) and MODIS-EVI2, VIIRS-EVI2, and PhenoCam-GCC (GCC T50, T25, and T10 representing 50th, 25th, and 10th percentiles of greenness falling)-derived phenometrics

		MODIS—Leaf fall Senescence			VIIRS—Leaf fall Senescence			GCC—Leaf fall			
<b>Error estimate</b>	Phenesse estimate	Start	Mid	End	Start	Mid	End	T50	T25	T10	
RMSE	Est_05	24.5**	33.7**	74.0**	25.4	36.0	67.1	54.4	67.9	72.2	
	Est_50	56.9*	16.2*	34.4*	49.8	18.5	27.9	25.4	25.3	28.3	
	Est_95	82.0	38.4	13.5	73.7	38.5	10.9	37.5	17.6	13.8	
MBE	Est_05	-16.9**	27.3**	70.9**	-8.9	26.5	61.0	44.5	61.9	66.6	
	Est_50	<b>-55.4*</b>	-11.1*	32.5*	-47.3	-11.9	22.5	1.3	18.7	23.4	
	Est_95	-80.2	-35.9	7.7	-72.1	-36.7	-2.2	-27.2	-9.8	-5.1	

Notes: No statistically significant relationships were recorded. Bold text indicates statistically significant regression relationships at \*p < 0.05; \*\*p < 0.01; \*\*\*p < 0.001.

leaves were statistically significantly (p < 0.01) correlated with VIIRS-derived spring phenometrics (greenup, midgreen, and maturity) whereas later in situ phenesse estimates (95th percentile dates) were significantly (p < 0.01)

correlated with VIIRS-derived autumn phenometrics (start, mid, and end of senescence) (Tables 11 and 12, Figure S6). Overall, the strongest agreement between in situ estimates of leaves and VIIRS-derived spring

ECOSPHERE 19 of 25

**TABLE 11** Regression relationships between phenesse estimates (DOY) of in situ phenology and VIIRS-EVI2-derived spring phenometrics (DOY) across all species, sites, and years

	VIIRS green-up			VIIRS mid-green			VIIRS maturity		
In situ phenesse estimates	p	Slope	R <sup>2</sup>	p	Slope	R <sup>2</sup>	p	Slope	$R^2$
Early phenophases									
$P_5$	0.774	0.078	0.003	0.574	0.232	0.026	0.005	2.931	0.210
P <sub>50</sub>	0.283	-0.268	0.034	0.343	-0.362	0.009	0.292	1.072	0.033
Leaves									
$P_5$	0.001	1.502	0.343	0.000	1.697	0.382	0.000	3.944	0.410
P <sub>50</sub>	0.003	1.331	0.267	0.002	2.154	0.299	0.000	5.636	0.407

*Notes*: Early phenophases include breaking leaf bud, breaking needle bud, emerging needles, and initial growth. The phenophase leaves indicates one or more unfolded leaves present.  $P_5$ , and  $P_{50}$  refer to the dates corresponding to the 5th and 50th percentiles of phenesse estimates, respectively. The p values in boldface are significant at the 0.05 level. Corresponding scatterplots available in Appendix S1: Figure S6.

**TABLE 12** Regression relationships between phenesse estimates (DOY) of in situ phenology and VIIRS-EVI2-derived autumn phenometrics (DOY) across all species, sites, and years

	VIIRS start- senescence			VIIRS mid-senescence			VIIRS end-senescence		
In situ phenesse estimates	p	Slope	R <sup>2</sup>	p	Slope	$R^2$	p	Slope	$R^2$
Leaf color									
$P_5$	0.999	0.001	0.000	0.971	0.021	0.000	0.488	-0.664	0.038
P <sub>50</sub>	0.994	0.002	0.000	0.915	-0.037	0.001	0.459	-0.416	0.043
P <sub>95</sub>	0.997	0.001	0.000	0.774	-0.081	0.007	0.673	-0.197	0.014
Leaf fall									
$P_5$	0.089	0.876	0.206	0.118	1.250	0.178	0.579	-0.792	0.024
P <sub>50</sub>	0.128	0.440	0.169	0.183	0.607	0.132	0.576	-0.443	0.025
P <sub>95</sub>	0.479	0.127	0.039	0.631	0.149	0.018	0.749	-0.152	0.008
Leaves									
$P_{95}$	0.000	2.448	0.382	0.000	3.998	0.493	0.000	5.732	0.521

*Notes*: The phenophase leaves indicates one or more unfolded leaves present.  $P_{95}$  refers to the date corresponding to the 95th percentile of phenesse estimates. The p values in boldface are significant at the 0.05 level. Corresponding scatterplots available in Appendix S1: Figure S6.

phenometrics was between early (5th percentile) estimates of leaves and VIIRS greenup with an RMSE of 28.4 days and an MBE of -1.2 days (Table 6). In autumn, strongest agreement was between late (95th percentile) estimates of leaves and VIIRS-mid-senescence dates with an RMSE of 59.9 days and an MBE of 5.2 days (Table 8).

PhenoCam GCC-derived phenometrics showed a similar correlation pattern with the timing of spring and autumn in situ phenophase estimates as MODIS-and VIIRS-derived phenometrics (Tables 5, 6, 8–10, 13, and 14). In situ estimates of leaves in spring (5th and 50th percentile dates) and autumn (95th percentile dates) were statistically significantly correlated (p < 0.000) with corresponding GCC-derived spring and autumn phenometrics. The strongest relationship in spring was between the 5th percentile phenophase estimates of

leaves and GCC T10 (10th percentile greenness rising) with an RMSE of 24.1 days and an MBE of 11.9 days; and the best relationship in autumn was between the 95th percentile phenophase estimates of leaves and GCC T25 (25th percentile greenness falling) with an RMSE of 37.1 days and an MBE of -1.9 days (Tables 5, 6, and 8-10, Appendix S1: Figure S7).

# Correlation between satellite and PhenoCam-derived phenological time series

At all sites, apart from ONAQ, lag correlation analyses revealed a tendency for EVI2 to show stronger correlation, than NDVI, with GCC as indicated by higher

**TABLE 13** Regression relationships between phenesse estimates (DOY) of in situ phenology and PhenoCam-GCC-derived spring (GCC T10, T25, and T50 representing 10th, 25th, and 50th percentiles of greenness rising) phenometrics (DOY) across all species, sites, and years

	GCC T10			GCC T25			GCC T50		
In situ phenesse estimates	p	Slope	$R^2$	p	Slope	$R^2$	p	Slope	$R^2$
Early phenophases									
$P_5$	0.006	0.816	0.210	0.125	0.503	0.072	0.986	0.006	0.000
$P_{50}$	0.000	0.728	0.324	0.027	0.509	0.143	0.326	0.231	0.030
Leaves									
$P_5$	0.000	1.389	0.746	0.000	1.644	0.704	0.000	1.979	0.598
P <sub>50</sub>	0.000	2.178	0.927	0.000	2.636	0.915	0.000	2.300	0.842

Notes: Early phenophases include breaking leaf bud, breaking needle bud, emerging needles, and initial growth. Leaves indicate one or more unfolded leaves present.  $P_5$  and  $P_{50}$  refer to the dates corresponding to the 5th and 50th percentiles of phenesse estimates, respectively. The p values in boldface are significant at the 0.05 level. Corresponding scatterplots available in Appendix S1: Figure S7.

**TABLE 14** Regression relationships between phenesse estimates (DOY) of in situ phenology and PhenoCam-GCC-derived autumn (GCC T50, T25, and T10 representing 50th, 25th, and 10th percentiles of greenness falling) phenometrics (DOY) across all species, sites, and years

·									
	Start-senescence, GCC T50			Mid-senescence, GCC T25			End-senescence, GCC T10		
In situ phenesse estimates	p	Slope	R <sup>2</sup>	p	Slope	R <sup>2</sup>	p	Slope	$R^2$
Leaf color									
$P_5$	0.809	-0.079	0.009	0.686	-0.274	0.025	0.686	-0.327	0.025
P <sub>50</sub>	0.404	-0.134	0.101	0.506	-0.224	0.066	0.588	-0.219	0.044
P <sub>95</sub>	0.225	-0.164	0.202	0.575	-0.164	0.047	0.740	-0.117	0.017
Leaf fall									
P <sub>5</sub>	0.622	-0.255	0.037	0.681	0.442	0.106	0.721	0.458	0.019
P <sub>50</sub>	0.947	-0.017	0.001	0.970	0.021	0.000	0.951	0.039	0.001
P <sub>95</sub>	0.144	-0.198	0.279	0.393	-0.253	0.026	0.527	-0.226	0.059
Leaves									
$P_{95}$	0.000	0.910	0.674	0.000	0.897	0.710	0.000	0.905	0.710

*Notes*: Leaves indicates one or more unfolded leaves present.  $P_{95}$  refer to the date corresponding to the 95th percentile of phenesse estimates. The p values in boldface are significant at the 0.05 level. Corresponding scatterplots available in Appendix S1: Figure S7.

correlation coefficients. This pattern was particularly noticeable at sites where evergreen vegetation was present (Figure 8c,e). The highest correlations between satellite phenometrics and GCC were obtained at HARV, a deciduous broadleaf forest. Overall, there was no evidence of a significant lag between PhenoCam-GCC- and satellite-derived phenometrics.

### DISCUSSION

Summarizing the number of days discrepancy between in situ- and RS-derived phenometrics reported in the literature was challenging due to the range of methods (satellite, PhenoCam, C flux), species, ecosystems, locations, observation durations, and error measure (RMSE, MBE, or MAE) reported in the various studies (Table 1). In addition, quantifying discrepancies between different methods was also hindered by a lack of colocated data collection methods at any one site. Even though, in situ, PhenoCam, C flux, and a range of satellite data were available from which to determine phenometrics for each of the five NEON sites examined in this study, we still encountered challenges. For example, because of significant data gaps (due to initial setup of the flux towers) in both spring and autumn we were unable to calculate phenology transition dates from the C flux data at the selected sites. However, as the NEON project progresses,

ECOSPHERE 21 of 25

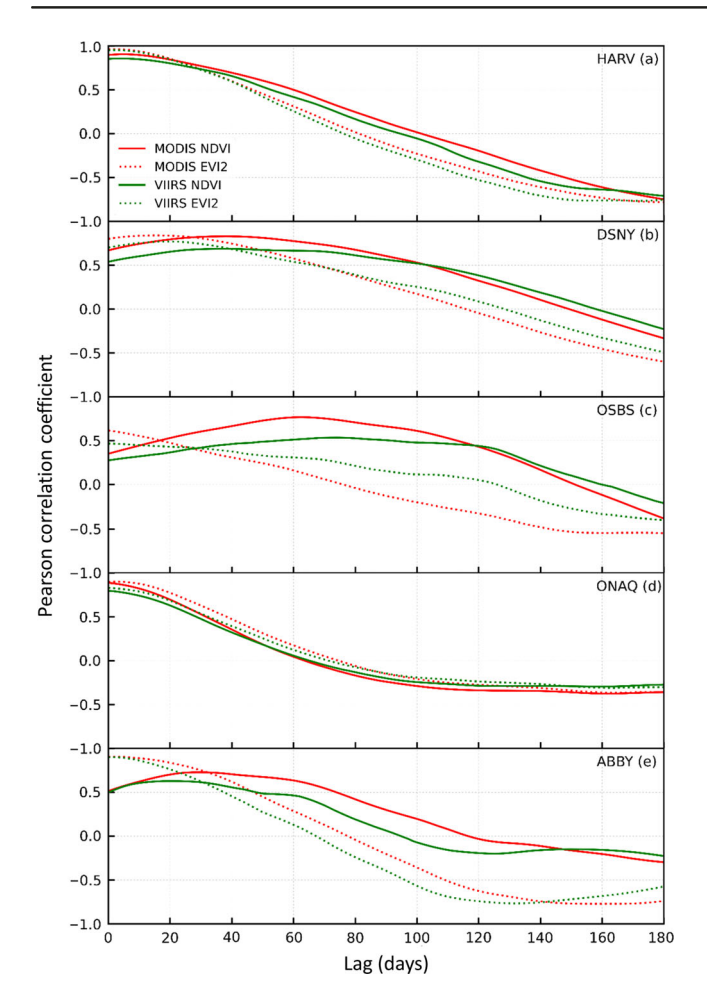


FIGURE 8 Pearson lag correlation coefficients between satellite-derived phenometrics (NDVI and EVI2) and GCC at five NEON sites. (a) HARV; Harvard Forest, MA; (b) DSNY; Disney Wilderness Preserve, FL; (c) OSBS; Ordway-Swisher Biological Station, FL; (d) ONAQ; Onaqui, UT; and (e) ABBY; Abby Road, WA

we expect data quality issues to be greatly reduced and the colocation of such a wide range of data collection methods will be invaluable to address complex ecological questions in future.

The literature review revealed that the timing of in situ budburst and GCC-derived SOS showed relatively close agreement for individual deciduous species, such as oak (RMSE: 3.6 days) (Keenan et al., 2014) and honey mesquite (RMSE: 8.6 days) (Browning et al., 2017) but not for the C4 grass, black grama (RMSE: 105.4 days) (Browning et al., 2017). However, at larger spatial scales such as plot and landscape levels agreement between in situ budburst and either C flux (mixed forest 8.6 days MAE) (Donnelly et al., 2019) or satellite-derived (NDVI or EVI) SOS (across a range of ecosystem types and regions 12–75 days MAE and RMSE) (Fu et al., 2014; Peng et al., 2017, 2018; Donnelly et al., 2019) was much weaker. Furthermore, satellite-derived LAI-SOS differed

from in situ budburst by 9 and 11 days (RMSE) across Europe and the United States, respectively (Bórnez et al., 2020). Comparison of RS-derived SOS such as between satellite (NDVI or EVI2) and PhenoCam (GCC or VCI) showed somewhat closer agreement than with in situ budburst especially for deciduous broadleaf forest (RMSE: 4-9 days) (Filippa et al., 2018; Richardson et al., 2018; Zhang et al., 2018a). However, discrepancies between satellite and C flux spring phenology across a range of ecosystems in the United States were large (RMSE: 17-54 days) (Peng et al., 2017). All the aforementioned discrepancies likely related, primarily to, the range of parameters being monitored whether in situ observations, leaf spectral properties at a range of scales (satellite and PhenoCam) or photosynthetic activity (flux tower gross primary productivity).

There were fewer reports (in the literature review) of autumn phenophases than spring phenophases (Table 1). But there was slightly weaker agreement between in situ and RS phenometrics for autumn. Keenan et al. (2014) reported a 2.5 days (RMSE) discrepancy between in situ leaf color and GCC-derived EOS for oak while Browning et al. (2017) reported 24 days (RMSE) and 16 days (RMSE) difference for black grama and honey mesquite, respectively, for the same phase. Discrepancies between satellite-derived (EVI2 and NDVI) EOS and in situ leaf color and leaf fall of temperate deciduous trees was 20 days (MAE) and 24 days (MAE), respectively, in Ireland (Donnelly et al., 2018) and approximately 7 and 12 days (MAE) in northern Wisconsin, USA (Zhou et al., 2020). However, discrepancies between net ecosystem exchange and in situ autumn phenology in northern Wisconsin was much greater (MAE: 1-83 days) (Table 1). In contrast to spring phenology satellite-derived LAI-EOS differed greatly from in situ autumn color by 28 days and 25 days (RMSE) across Europe and the United States, respectively (Bórnez et al., 2020). Comparison between satellite (EVI and NDVI) and PhenoCam (VCI and GCC)-derived EOS ranged between 7 and 35 days (RMSE) depending on the ecosystem in question (Table 1) (Browning et al., 2017; Filippa et al., 2018; Richardson et al., 2018; Zhang et al., 2018a). As with spring phenology, discrepancies may be attributed to different methods observing different parameters, differences in ecosystem, landscape heterogeneity, scale, and species being observed.

While examining the in situ observations at the five NEON sites in the current study it became apparent, in some instances, that the DOY on which leaf color and leaf fall were recorded were often the same day for both phenophases and also for different species. This date may have been the last day of the autumn observation campaign and may not be a true reflection of the actual last

day on which these phenophases occurred. This raises the concern that a fixed term observation period runs the risk of excluding early and/or late phenophase dates at the extremes of the growing season and may not be suitable in the long-term to capture the gradual shift toward earlier spring and later autumn phenophases. Therefore, to address this issue in future, regular monitoring using PhenoCam photos could help inform and facilitate a more flexible start/end date to the in situ observation campaign rather than having to implement continuous year-round phenological observations. Another common but challenging issue for in situ phenological networks relates to the choice of species to observe which will ultimately be determined by the research question being addressed by the phenological data. The species choice at the NEON sites examined here tracked the satellite and PhenoCam vegetation signal fairly well with the slight exception of DSNY. At this site, the PhenoCam GCC exhibited a clear rise and fall in greenness which was not evident in the in situ phenophase data suggesting that perhaps other species or phenophases which were not recorded may be driving the GCC signal.

Annual phenological profiles, for both in situ and RS methods, exhibited considerable intersite variation reflective of the local vegetation type at each of the five NEON sites examined. For the most part, the dominant species being monitored for in situ phenology was reflected in the PhenoCam GCC annual profile, even at sites with a year-round growing season (OSBS and DSNY). The phenological profile of the deciduous species (C. cornuta) at ABBY appeared to be masked by the evergreen species which dominated the satellite and near-ground camera signals, both of which showed close year-round agreement. Overall, compared to GCC, the annual MODISand VIIRS-EVI2 profiles showed less clearly defined spring and autumn transitions reflective of the in situ phenology. The reasons are likely due to a combination of factors, including, relative abundance and dominance of the species being observed in the in situ campaign and the large spatial scale of the satellite pixels which integrate a much broader vegetation signal outside the FOV of the PhenoCam in which many of the in situ observations were collected.

We used phenesse estimates of in situ phenology for comparison with RS phenometrics because they have the advantage of using presence-only data to estimate dates of specific phenophases using a parametric bootstrapping approach to estimate any percentile based on the Weibull distribution (Belitz et al., 2020). This approach enhanced our ability to use NEON in situ phenological observations because it allowed phenological estimates to be made outside of the observation periods, which was essential given the fixed term observation periods observed in our in situ

dataset. Even though early spring phenophase (breaking leaf bud, breaking needle bud, emerging needles, and initial growth) estimates (5th percentile dates) were statistically significantly correlated with MODIS greenup, VIIRS maturity, and GCC greenness rising (10th percentile) dates, the RS dates were 23, 58, and 49 days later, respectively, than in situ phenology resulting in very large discrepancies. However, discrepancies between MODIS greenup and GCC greenness rising (10th percentile) dates and the estimate of early (50th percentile) spring phenophases were greatly reduced at 9 and 11 days, respectively. These results suggest that satellite and PhenoCam phenometrics can reasonably capture early in situ spring phenology once roughly 50% of the vegetation has reached this phase but earlier phenology (5th percentile dates) still proves difficult to capture using RS technologies. The discrepancies reported here, for early spring in situ versus GCC, are slightly higher than those reported for C3 species in the literature (Browning et al., 2017; Keenan et al., 2014). However, both Keenan et al. (2014) and Browning et al. (2017) reported on individual species at a particular location whereas our results are reflective of a number of species representing a range of plant functional groups and ecosystem types, which likely accounts for some of the differences.

The phenophase "leaves" refers to the phase when one or more fully unfolded leaves are visible on the plant being observed. Therefore, when observers record "yes," for this phase, for the first time in the season, it marks the beginning of leaf-out and when they stop recording "yes" then leaf-fall has been reached. Phenesse estimates of "leaves" proved very useful in determining the start (5th percentile dates) and end (95th percentile dates) of spring and autumn, respectively. Overall, the timing of early leaves estimates (5th percentile dates) showed significant relationships with early RS phenometrics whereas the later leaves estimates (95th percentile dates) were strongly correlated with RS senescence phenology. However, the GCC transition dates for end of greenness falling (T10) were closer (RMSE/MBE: 37 days/2.8 days) to the timing of end of leaves (phenesse 95th percentile dates) than to the satellite-derived end of senescence (RMSE: 49.2-73.8 days/MBE: 18.3-40.8 days). This was not surprising, given the higher resolution of the PhenoCam compared to the satellite sensors, and agrees with previous studies (Browning et al., 2017; Keenan et al., 2014). In general, RS phenometrics showed better agreement with phenesse estimates of the timing of first reporting of leaves in spring with smaller RMSE/MBE, compared to earlier spring phenophases; but it was not the case for autumn. PhenoCam transition dates proved to be closer to in situ estimates than the coarser resolution satellite data, as the camera is positioned closer to

ECOSPHERE 23 of 25

the ground, which greatly reduced systematic error associated with atmospheric effects and geometric distortion.

The analyses carried out in this study highlights the challenges of capturing in situ phenology with RS techniques even when data, for both methods, are available for the same site. Even though PhenoCams and satellites observe the spectral properties of vegetation and C flux measures productivity they are both reflective of ecosystem phenology. Therefore, in the coming decades, the high-intensity nature of data collection at NEON sites coupled with an increase in the number and type of the species observed will likely reduce the discrepancies reported here. The addition of more species will provide a more comprehensive phenological profile at the ecosystem level, which should better reflect the scale of the RS phenological signal.

# CONCLUSIONS

Despite the abundance of colocated data collection methods, by which to derive annual phenological profiles, across a range of vegetation types, facilitated by the NEON project, we encountered a number of technical and scalerelated challenges. Technical challenges included missing data due to intermittent instrumentation failure, such as with the carbon flux data, typical of the initial setup phase of such a large and complex project. The short duration of the time series' coupled with the small number of species available at each site meant that it was not statistically meaningful to examine relationships between in situ and RS phenometrics at the community level. Therefore, we could not determine if relationships between in situ and RS methods were more robust in some ecosystems compared to others. However, many of these issues will likely be overcome in the coming years as the project progresses and the infrastructure stabilizes resulting in more data becoming available. In general, neither satellite nor near-ground-derived phenometrics successfully captured the in situ phenology estimates at the NEON sites examined as indicated by large variation in RMSE of between 21.7 days and 92.7 days in spring and between 10.9 days and 110.8 days in autumn. In addition, MBE values ranged between -85.3 days and 78.4 days in spring and -75.9 days to 87.5 days in autumn. Overall, given the short duration of the time series, the inability to determine community level in situ phenology, mixed signals from satellite measurements and issues with upscaling, contributed to large discrepancies between in situ- and remotely derived phenometrics at the sites examined. Capturing in situ phenology using RS remains challenging, but as more colocated in situ and RS data becomes available at NEON (and other) sites and sensor technology advances, we will be better positioned to address this issue in future. In the

meantime, we encourage others to take on this intriguing challenge.

#### **ACKNOWLEDGMENTS**

The authors acknowledge support from the NEON Science Summit 2019 NSF Award #1906144. In addition, Alison Donnelly and Rong Yu are colead authors and were supported by a University of Wisconsin-Milwaukee Research Growth Initiative Grant (101x368). NEON is a program sponsored by the National Science Foundation and operated under cooperative agreement by Battelle. This material is based in part on work supported by the National Science Foundation through the NEON Program.

### **CONFLICT OF INTEREST**

The authors declare no conflict of interest.

#### ORCID

Alison Donnelly https://orcid.org/0000-0001-7101-2437

Katharyn Duffy https://orcid.org/0000-0001-6108-7718

Bijan Seyednasrollah https://orcid.org/0000-0002-5195-2074

Daijiang Li https://orcid.org/0000-0002-0925-3421

Kai Zhu https://orcid.org/0000-0003-1587-3317

#### REFERENCES

Belitz, M.W., E.A. Larsen, L. Ries, and R.P. Guralnick. 2020. "The Accuracy of Phenology Estimators for Use with Sparsely Sampled Presence-Only Observations." *Methods in Ecology and Evolution* 11(10): 1273–85. https://doi.org/10.1111/2041-210X. 13448

Bórnez, K., A. Descals, A. Verger, and J. Peñuelas. 2020. "Land Surface Phenology from VEGETATION and PROBA-V Data. Assessment over Deciduous Forests." *International Journal of Applied Earth Observation and Geoinformation* 84: 101974. https://doi.org/10.1016/j.jag.2019.101974

Browning, D.M., J.W. Karl, D. Morin, A.D. Richardson, and C.E. Tweedie. 2017. "Phenocams Bridge the Gap between Field and Satellite Observations in an Arid Grassland Ecosystem." *Remote Sensing* 9: 1071.

Cong, N., S.-L. Piao, A.-P. Chen, X.-H. Want, X. Lin, S.-P. Chen, S.-J. Han, G.-S. Shou, and A.-P. Zhang. 2012. "Spring Vegetation Green-Up Date in China Inferred from SPOT NDVI Data: A Multiple Model Analysis." Agricultural and Forest Meteorology 165: 104–13.

Delbart, N., E. Beaubien, L. Kergot, and T. Le Toan. 2015. "Comparing Land Surface Phenology with Leafing and Flowering Observations from the PlantWatch Citizen Network." *Remote Sensing of Environment* 160: 273–80.

Denny, E.G., K.L. Gerst, A.J. Miller-Rushing, G.L. Tierney, T.M. Crimmins, C.A.F. Enquist, P. Guertin, et al. 2014. "Standardized Phenology Monitoring Methods to Track Plant and Animal Activity for Science and Resource Management Applications." *International Journal of Biometeorology* 58: 591–601.

Donnelly, A., and R. Yu. 2017. "The Rise of Phenology with Climate Change: An Evaluation of IJB Publications." *International Journal of Biometeorology* 61: 29–50.

- Donnelly, A., L. Liu, X. Zhang, and A. Wingler. 2018. "Autumn Leaf Phenology: Discrepancies between *in Situ* Observations and Satellite Data at Urban and Rural Sites." *International Journal of Remote Sensing* 39: 8129–50.
- Donnelly, A., R. Yu, L. Liu, J.M. Hanes, L. Liang, M. Schwartz, and A.R. Desai. 2019. "Comparing *In Situ* Leaf Observations in Early Spring with Flux Tower CO<sub>2</sub> Exchange, MODIS EVI and Modeled LAI in a Northern Mixed Forest." *Agricultural and Forest Meteorology* 278: 107673. https://doi.org/10.1016/j.agrformet.2019.107673
- Elmendorf, S.C., K.D. Jones, B.I. Cook, F.M. Diez, C.A.F. Enquist, R. A. Bufft, M.O. Jones, et al. 2016. "The Plant Phenology Monitoring Design for the National Ecological Observatory Network." *Ecosphere* 7(4): e01303. https://doi.org/10.1002/ecs2.1303
- Elmore, A.J., C.D. Stylinski, and K. Pradhan. 2016. "Synergistic Use of Citizen Science and Remote Sensing from Continental-Scale Measurements of Forest Tree Phenology." *Remote Sensing* 8: 502. https://doi.org/10.3390/rs8060502
- Filippa, G., E. Cremonese, M. Migliavacca, M. Galvagno, O. Sonnentag, E. Humphreys, K. Hufkens, et al. 2018. "NDVI Derived from Near-Infrared-Enabled Digital Cameras: Applicability across Different Plant Functional Types." Agricultural and Forest Meteorology 249: 175–285.
- Fu, Y.H., S. Piao, M. Op de Beeck, N. Cong, H. Zhao, Y. Zhang, A. Menzel, and I.A. Janssens. 2014. "Recent Spring Phenology Shifts in Western Central Europe Based on Multiscale Observations." Global Ecology and Biogeography 23: 1255–63.
- Keenan, T.F., B. Darby, E. Felts, O. Sonnentag, M.A. Friedl, K. Hufkens, J. O'Keefe, et al. 2014. "Tracking Forest Phenology and Seasonal Physiology Using Digital Repeat Photography: A Critical Assessment." *Ecological Applications* 24(6): 1478–89.
- Melaas, E., M.A. Friedl, and A.D. Richardson. 2016. "Multiscale Modeling of Spring Phenology across Deciduous Forests in the Eastern United States." Global Change Biology 22: 792–805.
- Milliman, T., B. Seyednasrollah, A. M. Young, K. Hufkens, M. A. Friedl, S. Frolking, A. D. Richardson, et al. 2019. "PhenoCam Dataset v2.0: Digital Camera Imagery from the PhenoCam Network, 2000–2018". https://doi.org/10.3334/ornldaac/1689.
- Peng, D., C. Wu, C. Li, X. Zhang, Z. Liu, H. Ye, S. Luo, X. Liu, Y. Hu, and B. Fang. 2017. "Pring Green-up Phenology Products Derived from MODIS NDVI and EVI: Intercomparison and Validation Using National Phenology Network and AmeriFlux Observations." *Ecological Indicators* 77: 323–36.
- Peng, D., C. Wu, X. Zhang, L. Yu, A.R. Huete, F. Want, S. Luo, X. Liu, and H. Zhang. 2018. "Scaling up Spring Phenology Derived from Remote Sensing Images." *Agricultural and Forest Meteorology* 256–257: 207–19.
- Piao, S., Q. Liu, A. Chen, I.A. Janssens, Y. Fu, J. Dai, L. Liu, X. Lian, S. Shen, and X. Zhu. 2019. "Plant Phenology and Global Climate Change: Current Progresses and Challenges." *Global Change Biology* 25: 1922–40.
- Richardson, A.D., B.H. Braswell, D.Y. Hollinger, J.P. Jenkins, and S.V. Ollinger. 2009. "Near-Surface Remote Sensing of Spatial and Temporal Variation in Canopy Phenology." *Ecological Applications* 19: 1417–28.

- Richardson, A.D., T.A. Black, P. Ciais, N. Delbart, M.A. Friedl, N. Gobron, D.Y. Hollinger, et al. 2010. "Influence of Spring and Autumn Phenological Transitions on Forest Ecosystem Productivity." *Philossophical Transactions of the Royal Society of London. Series B, Biological Sciences* 365(1555): 3227–46.
- Richardson, A.D., K. Hufkens, T. Milliman, and S. Frolking. 2018. "Intercomparison of Phenological Transition Dates Derived from the PhenoCam Dataset V1.0 and MODIS Satellite Remote Sensing." *Scientific Reports* 8: 5679.
- Seyednasrollah, B., A.M. Young, K. Hufkens, T. Milliman, M.A. Friedl, A. Frolking, and A.D. Richardson. 2019a. "Tracking Vegetation Phenology across Diverse Biomes Using Version 2.0 of the PhenoCam Dataset." *Scientific Data* 6: 222. https://doi.org/10.1038/s41597-019-0229-9
- Seyednasrollah, B., A. M. Young, K. Hufkens, T. Milliman, M. A. Friedl, S. Frolking, A. D. Richardson, et al. 2019b. "PhenoCam Dataset v2.0: Vegetation Phenology from Digital Camera Imagery, 2000–2018." ORNL DAAC. https://doi.org/10.3334/ornldaac/1674.
- Seyednasrollah, B., T. Milliman, and A.D. Richardson. 2019c. "Data Extraction from Digital Repeat Photography Using xROI: An Interactive Framework to Facilitate the Process." *ISPRS Journal of Photogrammetry and Remote Sensing* 152: 132–44.
- Soudani, K., G. Le Marie, E. Dufrêne, C. Francois, N. Delpierre, E. Ulrich, and S. Cecchini. 2008. "Evaluation of the Onset of Green-Up in Temperate Deciduous Broadleaf Forests Derived from Moderate Resolution Imaging Spectroradiometer (MODIS) Data." Remote Sensing of Environment 112: 2643–55.
- Tang, J., C. Körner, H. Muraoka, S. Piao, M. Shen, S.J. Thackeray, and X. Yang. 2016. "Emerging Opportunities and Challenges in Phenology: A Review." *Ecosphere* 7: e01436.
- Wallace, C.S.A., J.J. Walker, S.M. Skirvin, C. Patrick-Birdwall, J.F. Weltzin, and H. Raichle. 2016. "Mapping Presence and Predicting Phenological Status of Invasive Buffelgrass in Southern Arizona Using MODIS, Climate and Citizen Science Observation Data." Remote Sensing 8: 524. https://doi.org/10.3390/rs8070524
- Wang, C., and K. Zhu. 2019. "Misestimation of Growing Season Length Due to Inaccurate Construction of Satellite Vegetation Index Time Series." *IEEE Geoscience and Remote Sensing Letters* 16(8): 1185–9. https://doi.org/10.1109/LGRS.2019.2895805
- White, M.A., K. de Beurs, K. Didan, D. Inouye, A. Richardson, O. Jensen, J. O'Keefe, et al. 2009. "Intercomparison, Interpretation, and Assessment of Spring Phenology in North America Estimated from Remote Sensing from 1982–2006." Global Change Biology 15: 2335–59.
- Zhang, X., M.A. Friedl, C.B. Schaaf, A.H. Strahler, J.C.F. Hodges, F. Gao, B.C. Reed, and A. Huete. 2003. "Monitoring Vegetation Phenology Using MODIS." *Remote Sensing of Environment* 84: 471–5.
- Zhang, X., S. Jayavelu, L. Liu, M.A. Friedl, G.M. Henebry, Y. Liu, C.B. Schaaf, A.D. Richardson, and J. Gray. 2018a. "Evaluation of Land Surface Phenology from VIIRS Data Using Time Series of PhenoCam Imagery." Agricultural and Forest Meteorology 256–257: 137–49.
- Zhang, X., L. Liu, Y. Liu, S. Jayavelu, J. Wang, M. Moon, G.M. Henebry, M.A. Friedl, and C.B. Schaaf. 2018b. "Generation and Evaluation of the VIIRS Land Surface Phenology Product." Remote Sensing of Environment 216: 212–29.
- Zhang, X., M. Friedl, and G. Henebry. 2020. "VIIRS/NPP Land Cover Dynamics Yearly L3 Global 500m SIN Grid V001" [Data

ECOSPHERE 25 of 25

Set]. NASA EOSDIS Land Processes DAAC. https://doi.org/10.5067/VIIRS/VNP22Q2.001.

Zhou, B., A. Donnelly, and M. Schwartz. 2020. "Evaluating Autumn Phenology Derived from Field Observations, Satellite Data and Carbon Flux Measurements in a Northern Mixed Forest, USA." *International Journal of Biometeorology* 64: 713–27.

# SUPPORTING INFORMATION

Additional supporting information may be found in the online version of the article at the publisher's website.

How to cite this article: Donnelly, Alison, Rong Yu, Katherine Jones, Michael Belitz, Bonan Li, Katharyn Duffy, Xiaoyang Zhang, et al. 2022. "Exploring Discrepancies between in Situ Phenology and Remotely Derived Phenometrics at NEON Sites." *Ecosphere* 13(1): e3912. <a href="https://doi.org/10.1002/ecs2.3912">https://doi.org/10.1002/ecs2.3912</a>